Neutron scattering studies of quantum, and multiferroic transition metal oxides

Junghwa Kim

Condensed Matter Seminar
April 6, 2009

Outline

1. Magnetic structures of magnetoelectric multiferroics : YMn_2O_5
2. Magnetic excitations of quantum dimer on triangular lattice : $Ba_3Cr_2O_8$

$TbMnO_3$

Magnetic control of ferroelectric polarization

T. Kimura[1*], T. Goto[1], H. Shintani[1], K. Ishizaka[1], T. Arima[2] & Y. Tokura[1]

Nature **426**, 55 (2003)

M. Kenzelmann *et.al.* *PRL* **95**, 087206 (2005)

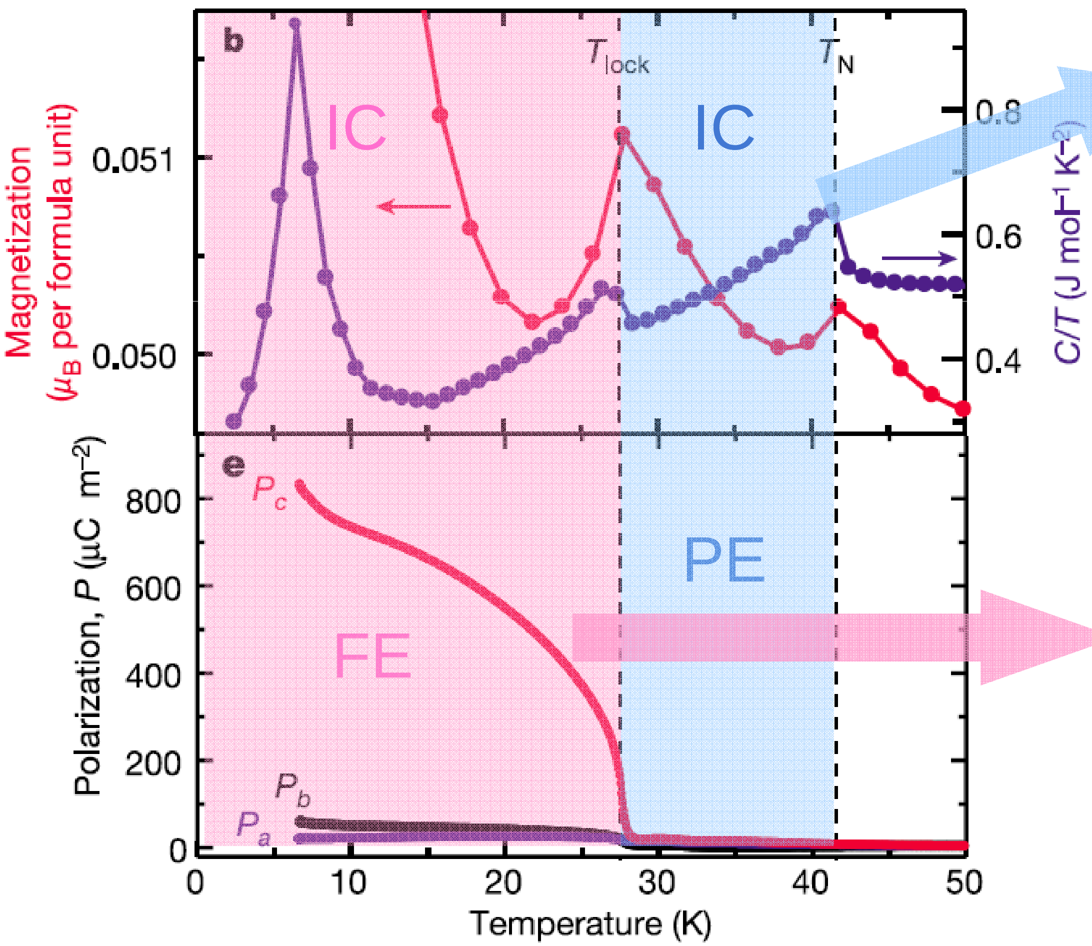

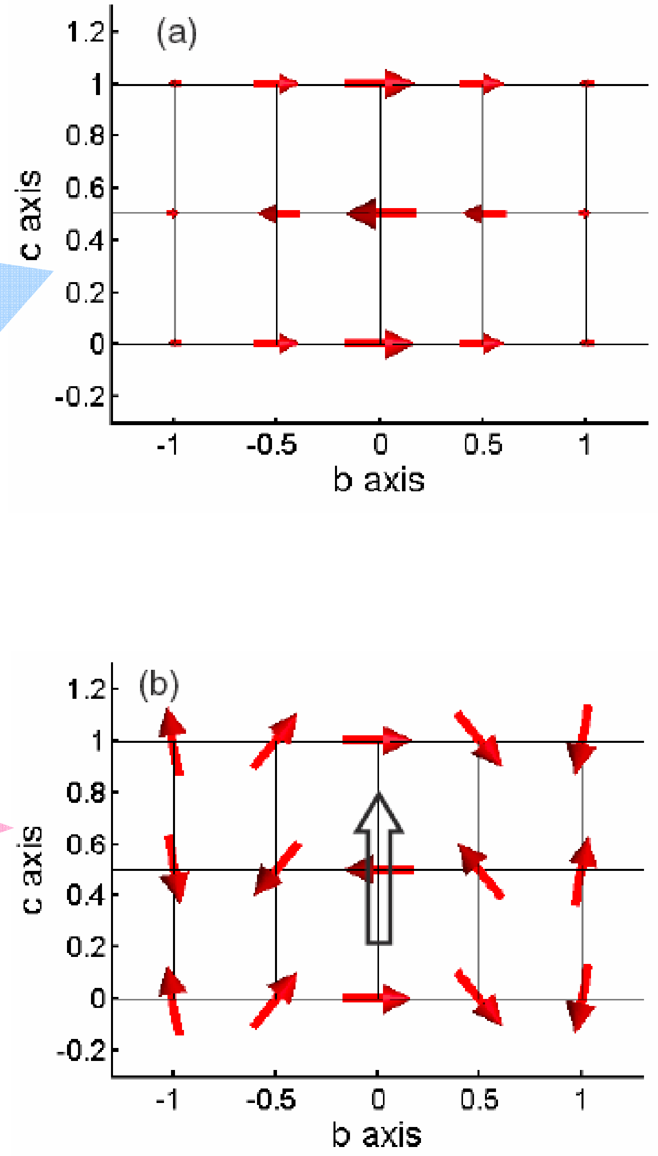

Magneto-electric coupling mechanism (I)

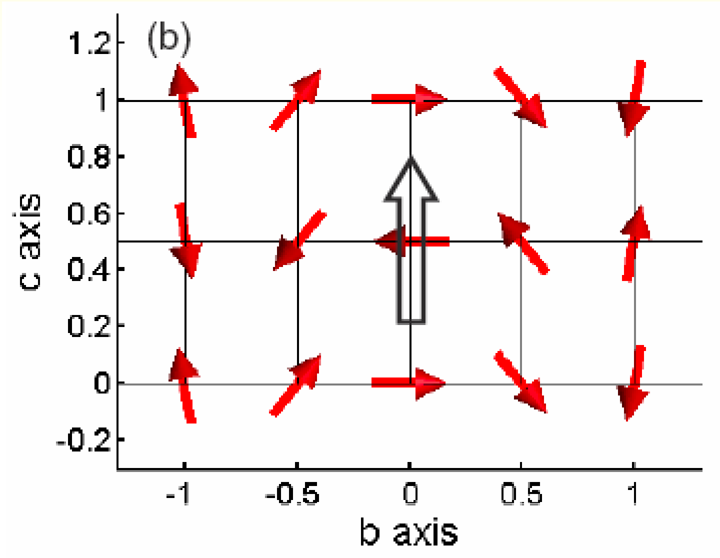

- incommensurate spiral spin structure

M. Kenzelmann *et.al. PRL* **95**, 087206 (2005)

- Spin-current mechanism : antisymmetric exchange coupling

  Mostovoy (*PRL* 2006), Katsura/Nagaosa/Balatsky (*PRL* 2005)

- Symmetry-based Ginzburg-Landau Theory

  A. B. Harris (*PRB* 2006)

YMn_2O_5

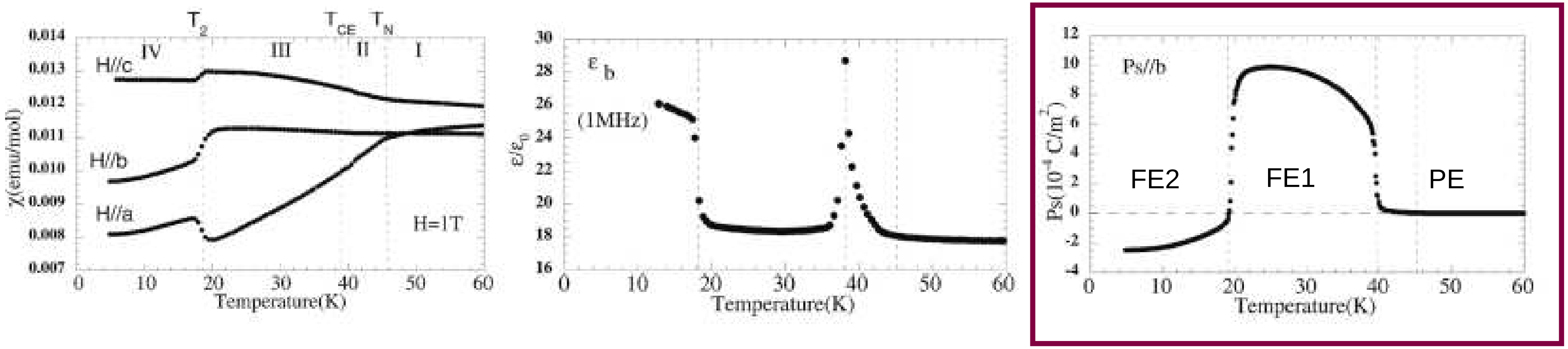

Y. Noda *et al. JKPS* **42**, 1192 (2003)

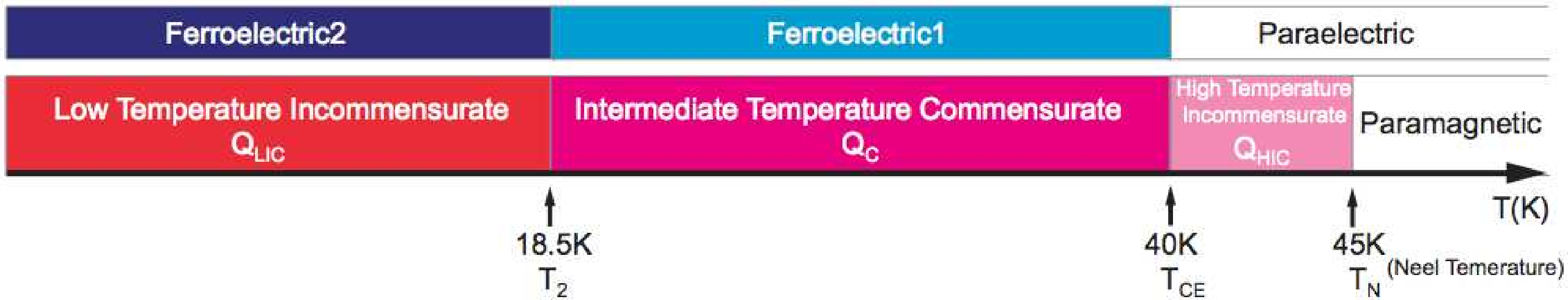

Crystal structure of YMn_2O_5

Crystal structure : Orthorhombic Space group : *Pbam*

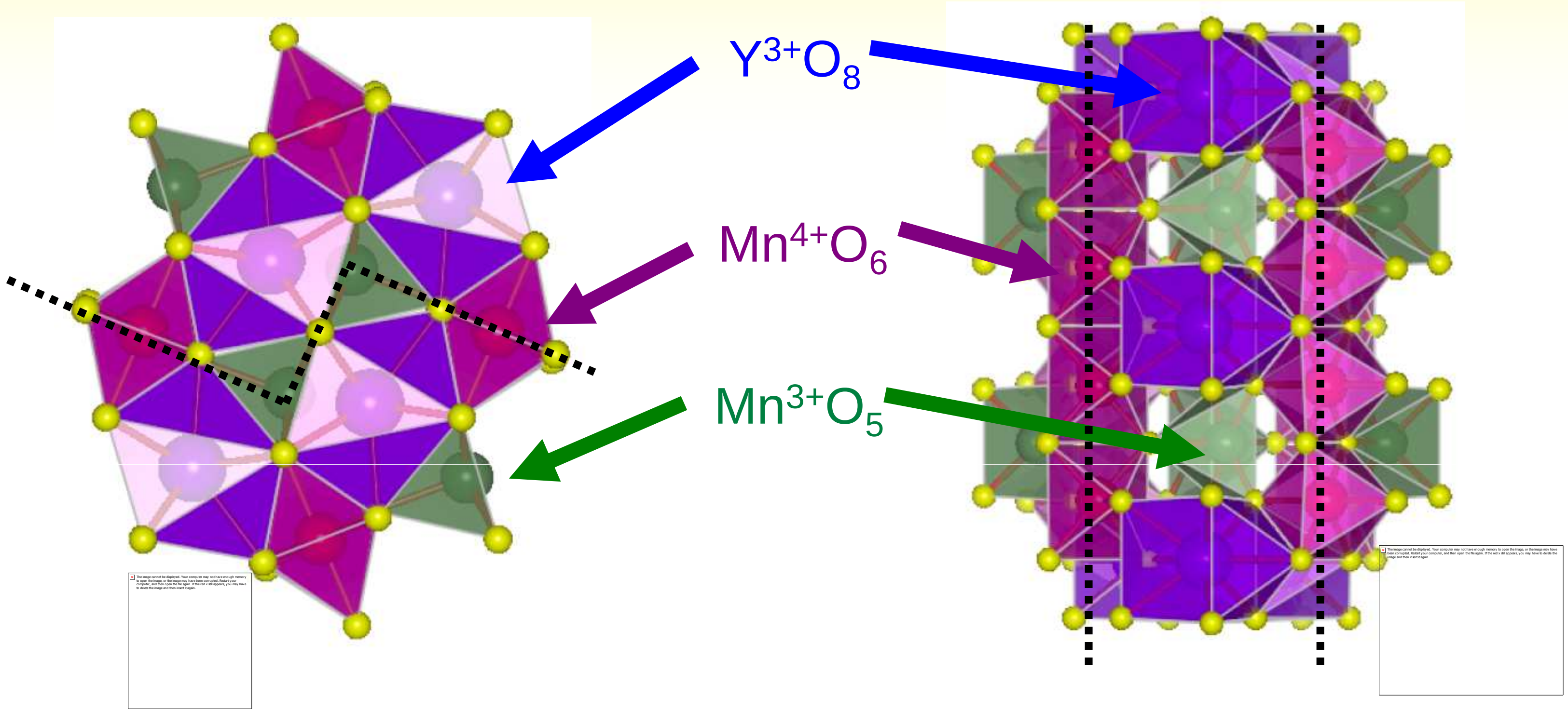

- edge sharing $Mn^{4+}O_6$ octahedra along the c-axis
- Mn^{3+}/Y^{3+}└ └ └ layers alternate along the c-axis
- neighboring $Mn^{3+}O_5$ pyramids share an edge
- neighboring $Mn^{4+}O_6$ octahedra share an edge
- neighboring $Mn^{3+}O_5$ and $Mn^{4+}O_6$ share a corner

YMn_2O_5

L.C. Chapon *et al.* *PRL* **96**, 097601 (2006)

Neutron powder diffraction

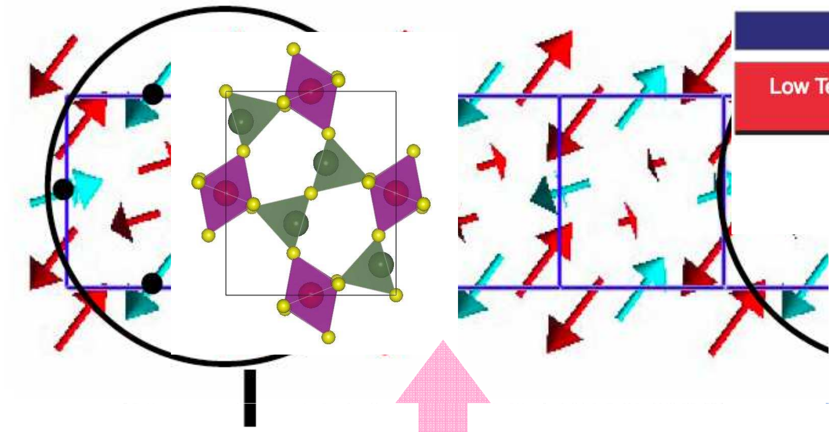

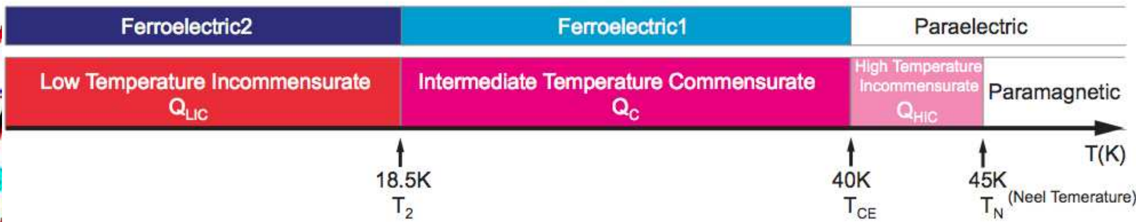

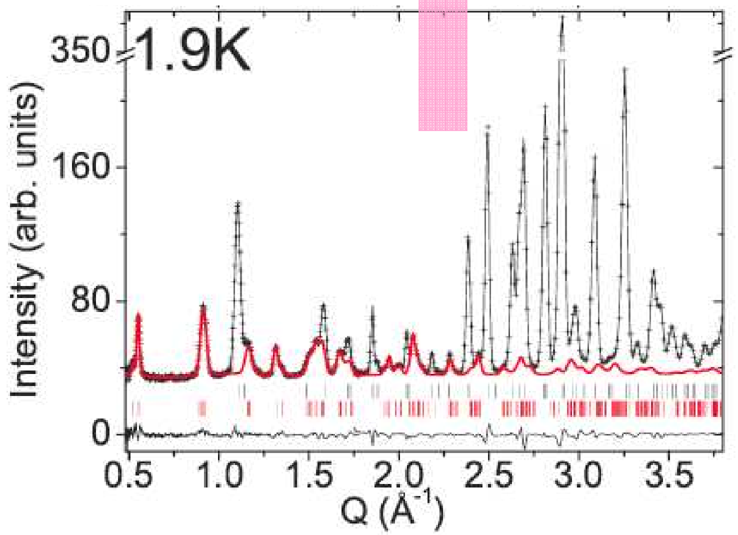

- Sinusoidal magnetic moments modulation along Mn^{3+}-Mn^{4+} zig-zag chain
- All spins lie on the ab-plane.
- Almost collinear AFM ordering along chains running along the a-axis.

- All spins lie on the ab-plane.
- Almost collinear AFM ordering along chains running along the a-axis.

- ++----++ arrangement along c.
- NO SPIRAL

Magneto-electric coupling mechanism (II)

- Magneto-elastic mechanism : symmetric exchange coupling

Mostovoy & Cheong (*Nature Materials* 2007)

YMn_2O_5

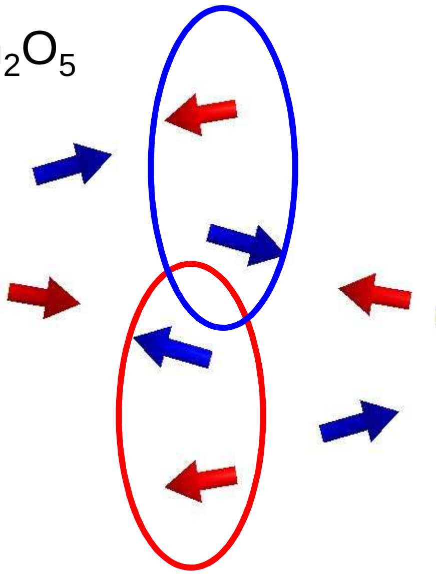

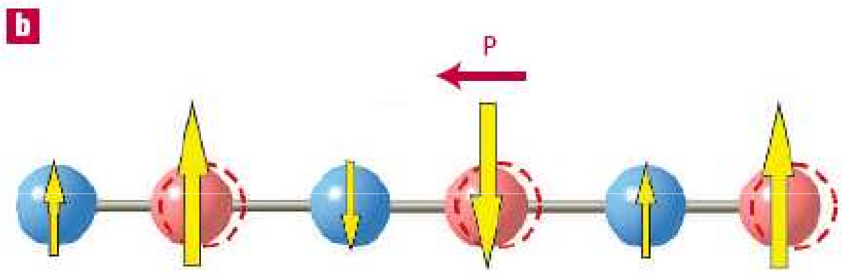

- Ions are shifted away from centrosymmetric positions by exchange striction, leading to electric polarization

Is the obtained model spin structure correct?

1. Can the model structure reproduce available diffraction data?
2. Is the model structure unique?

YMn_2O_5

Neutron powder diffraction

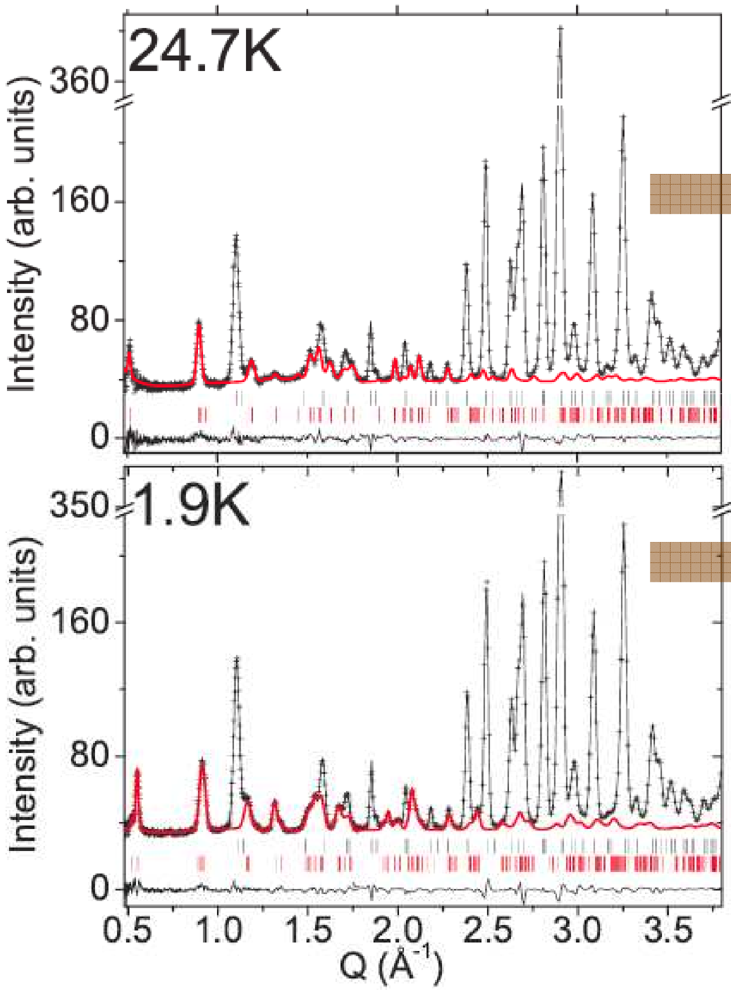

L.C. Chapon *et al. PRL* **96**, 097601 (2006)

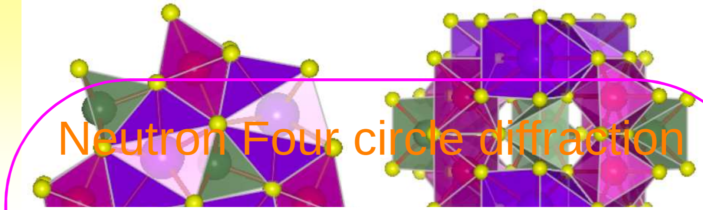

Neutron Four circle diffraction

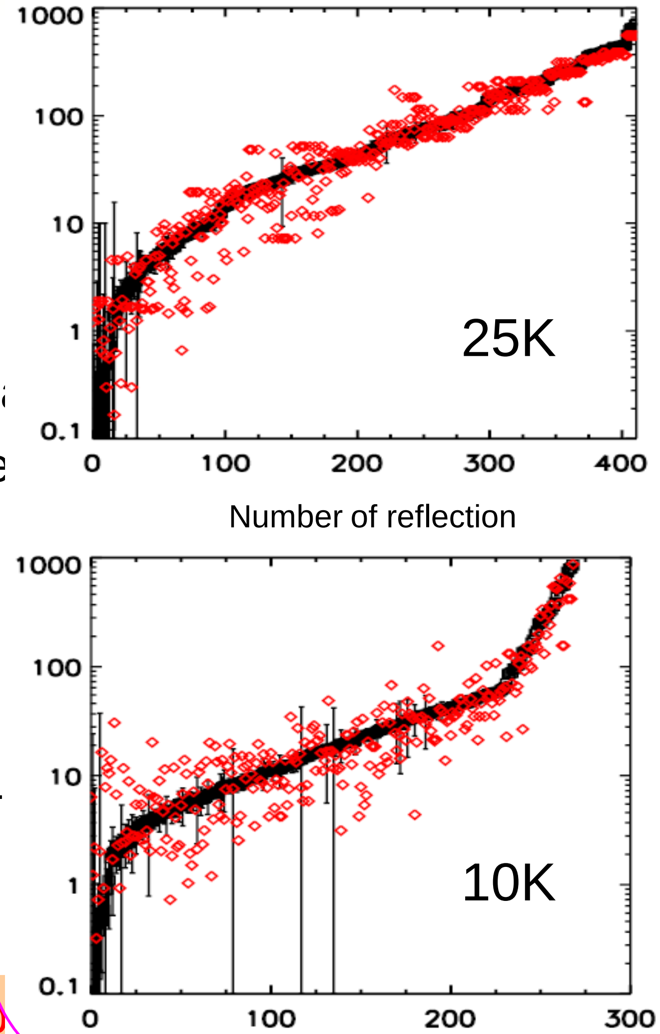

The ma

magne

48+1

Can p

complex spin structure correctly?

Experimental methods

- Single crystals (1g) of YMn_2O_5 were provided by S.-W. Cheong's group.
- Neutron Four-circle Diffraction (FCD) : **TriCS** at PSI (Switzerland)
- Polarized Neutron Diffraction (PND) : **NG-1** at NCNR (USA)

  CRYOPAD at JAEA (Japan)

TriCS

NG-1

CRYOPAD

Representation theory

In a material, the crystal symmetry restricts possible magnetic structures that the material order into. The space group of the magnetic structure, G_k, is a subgroup of the crystal symmetry group, G. And the possible spin structure is a linear combination of basis functions of the magnetic space group G_k.

For YMn_2O_5, G_k with k = (0.5,0,0.25) has two dimensional irreducible representations

Mn^{3+}

		(1)	(2)	(3)	(4)
τ_1^1	$\mathbf{k_1}$	1 0 0 0 0 0	1 0 0 0 0 0	0 0 0 i(1 0 0)	0 0 0 -i(1 0 0)
	$\mathbf{k_2}$	1 0 0 0 0 0	1 0 0 0 0 0	0 0 0 i(1 0 0)	0 0 0 -i(1 0 0)
τ_1^2	$\mathbf{k_1}$	0 1 0 0 0 0	0 1 0 0 0 0	0 0 0 -i(0 1 0)	0 0 0 i(0 1 0)
	$\mathbf{k_2}$	0 1 0 0 0 0	0 1 0 0 0 0	0 0 0 -i(0 1 0)	0 0 0 i(0 1 0)
τ_1^3	$\mathbf{k_1}$	0 0 1 0 0 0	0 0 -1 0 0 0	0 0 0 -i(0 0 1)	0 0 0 -i(0 0 1)
	$\mathbf{k_2}$	0 0 1 0 0 1	0 0 -1 0 0 0	0 0 0 -i(0 0 1)	0 0 0 -i(0 0 1)

$$
\begin{aligned}
\vec{S}(\vec{R},n) = & \{C^{11}\Psi_1^{k_1\tau_1^1} + C^{12}\Psi_2^{k_1\tau_1^1}\}\exp(i\vec{k_1}\cdot\vec{R}) + \{C^{13}\Psi_1^{k_2\tau_1^1} + C^{14}\Psi_2^{k_2\tau_1^1}\}\exp(i\vec{k_2}\cdot\vec{R}) \\
& +\{C^{21}\Psi_1^{k_1\tau_1^2} + C^{22}\Psi_2^{k_1\tau_1^2}\}\exp(i\vec{k_1}\cdot\vec{R}) + \{C^{23}\Psi_1^{k_2\tau_1^2} + C^{24}\Psi_2^{k_2\tau_1^2}\}\exp(i\vec{k_2}\cdot\vec{R}) \\
& +\{C^{31}\Psi_1^{k_1\tau_1^3} + C^{32}\Psi_2^{k_1\tau_1^3}\}\exp(i\vec{k_1}\cdot\vec{R}) + \{C^{33}\Psi_1^{k_2\tau_1^3} + C^{34}\Psi_2^{k_2\tau_1^3}\}\exp(i\vec{k_2}\cdot\vec{R}) \\
& +\{C^{41}\Psi_1^{k_1\tau_1^4} + C^{42}\Psi_2^{k_1\tau_1^4}\}\exp(i\vec{k_1}\cdot\vec{R}) + \{C^{43}\Psi_1^{k_2\tau_1^4} + C^{44}\Psi_2^{k_2\tau_1^4}\}\exp(i\vec{k_2}\cdot\vec{R}) \\
& +\{C^{51}\Psi_1^{k_1\tau_1^5} + C^{52}\Psi_2^{k_1\tau_1^5}\}\exp(i\vec{k_1}\cdot\vec{R}) + \{C^{53}\Psi_1^{k_2\tau_1^5} + C^{54}\Psi_2^{k_2\tau_1^5}\}\exp(i\vec{k_2}\cdot\vec{R}) \\
& +\{C^{61}\Psi_1^{k_1\tau_1^6} + C^{62}\Psi_2^{k_1\tau_1^6}\}\exp(i\vec{k_1}\cdot\vec{R}) + \{C^{63}\Psi_1^{k_2\tau_1^6} + C^{64}\Psi_2^{k_2\tau_1^6}\}\exp(i\vec{k_2}\cdot\vec{R})
\end{aligned}
$$

Intermediate Temperature Commensurate Phase (25K)

J.-H. Kim *et al. PRB* **78**, 245115 (2008)

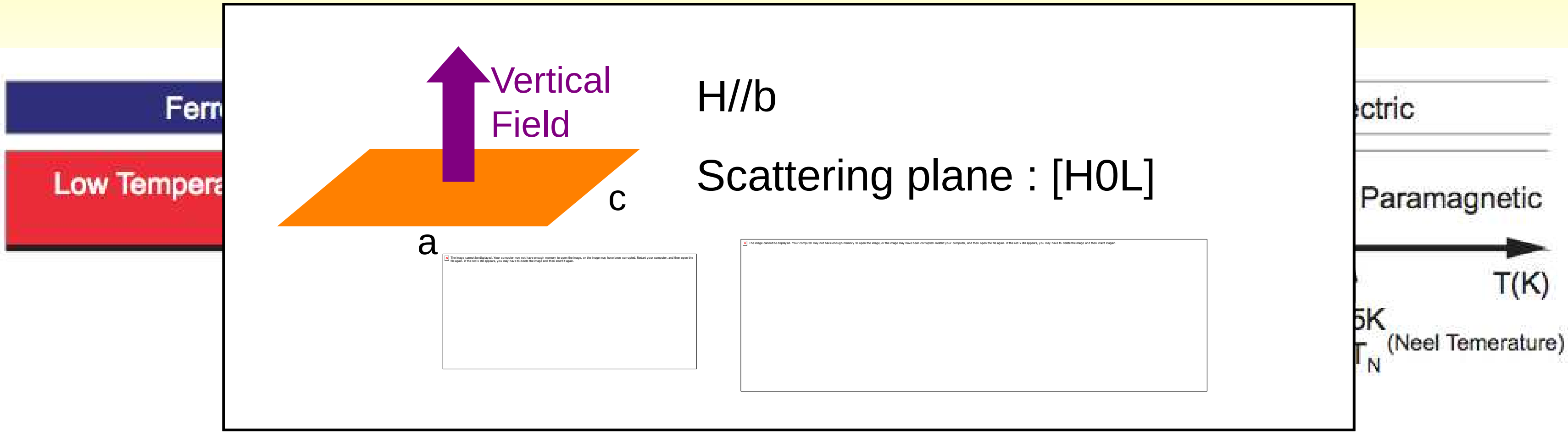

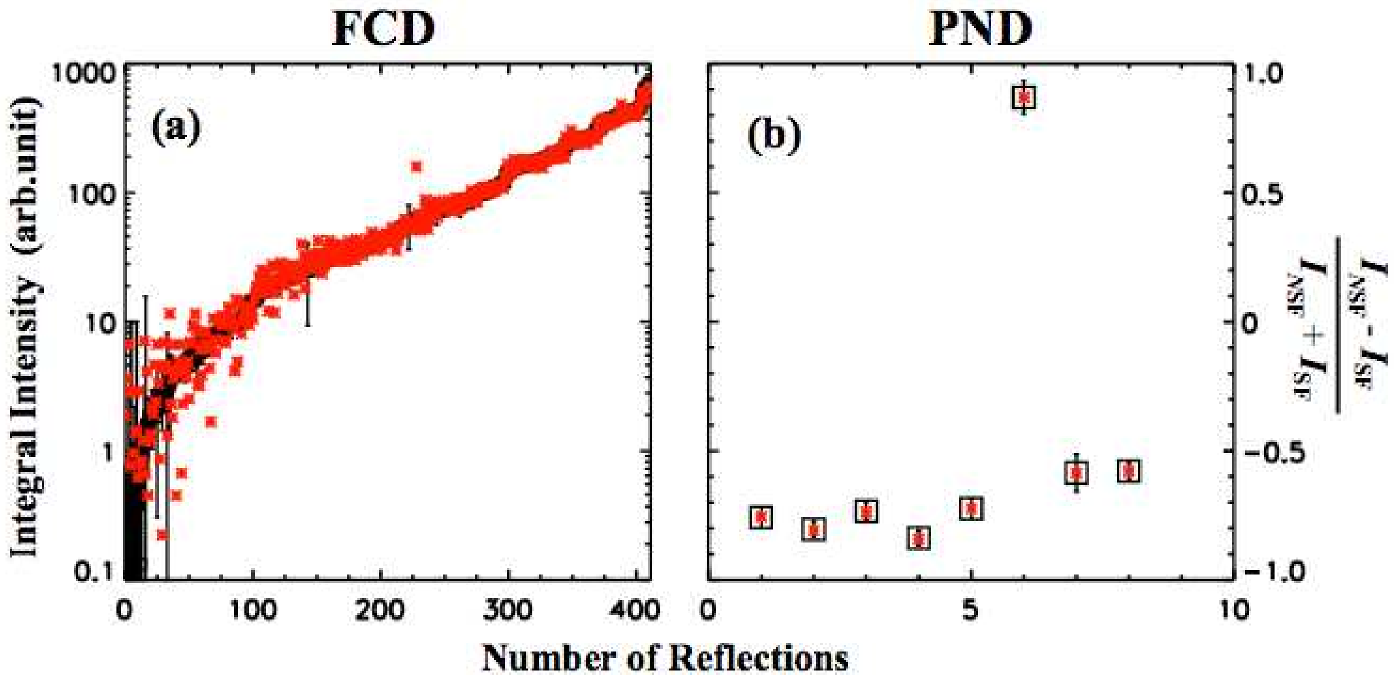

ITC (25K)

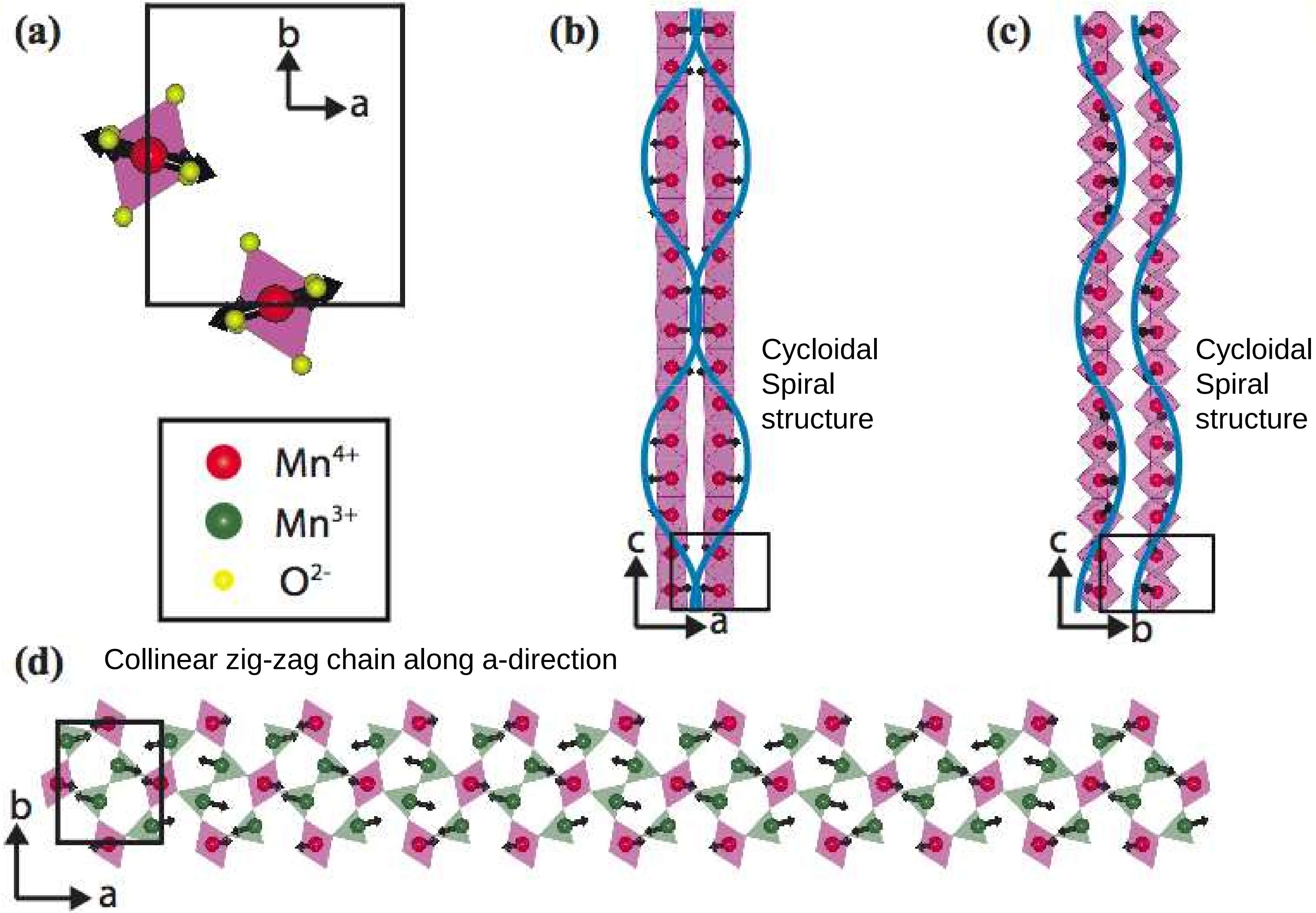

(a)
b
a
Mn^{4+}
Mn^{3+}
O^{2-}
(b)
Cycloidal
Spiral
structure
c
a
(c)
Cycloidal
Spiral
structure
c
b
(d)
Collinear zig-zag chain along a-direction
b
a

YMn_2O_5

L.C. Chapon *et al. PRL* **96**, 097601 (2006)

Neutron powder diffraction

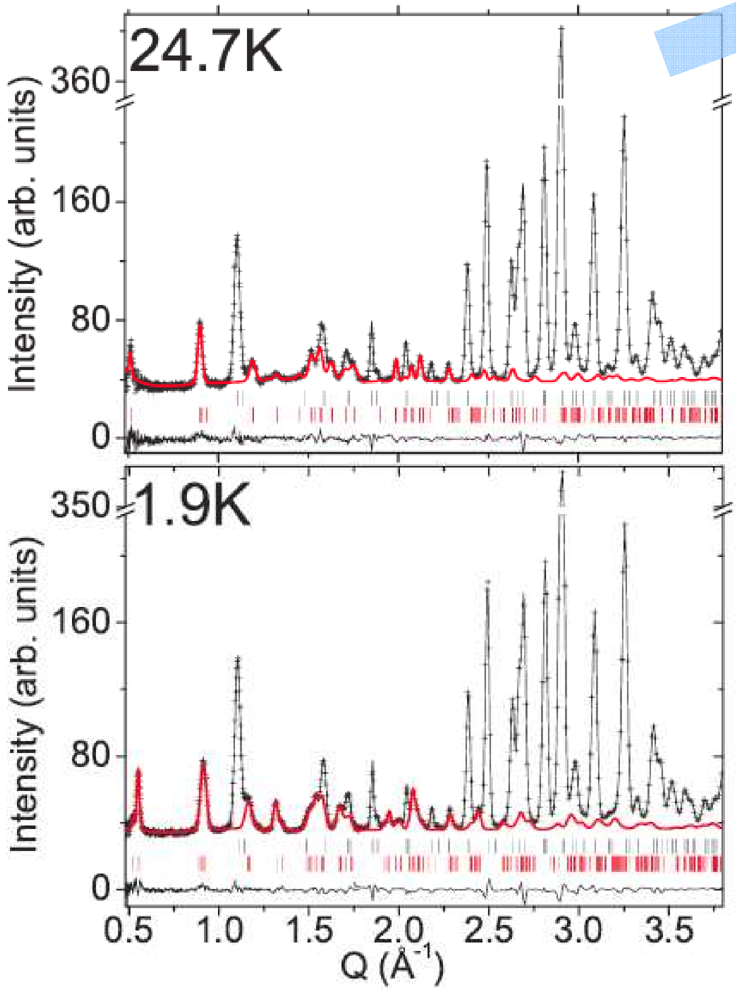

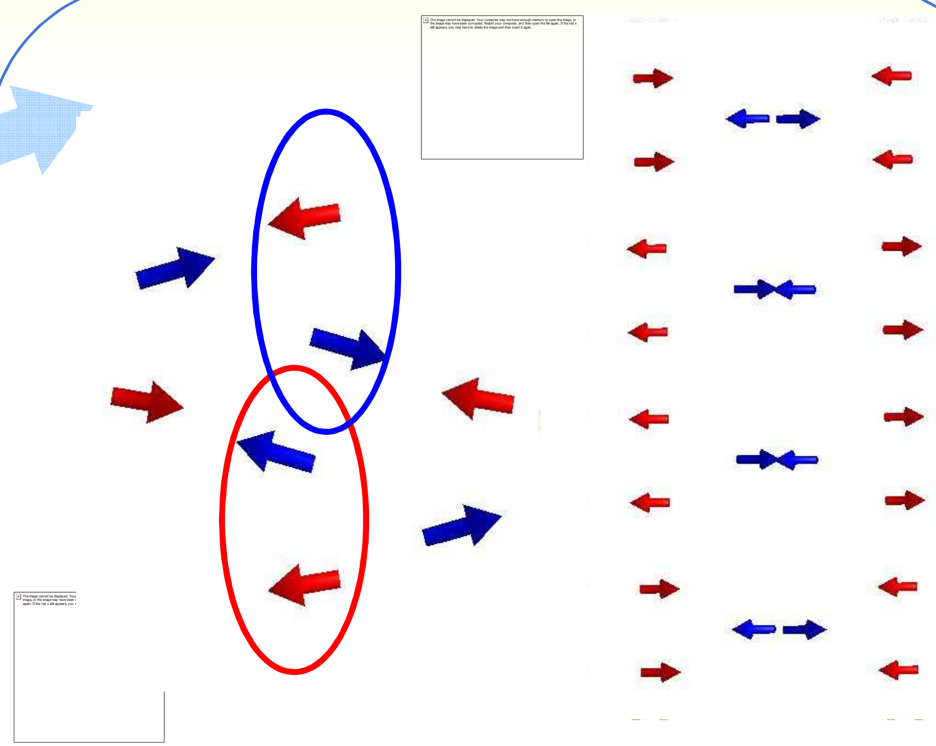

- NO SPIRAL

ITC (25K)

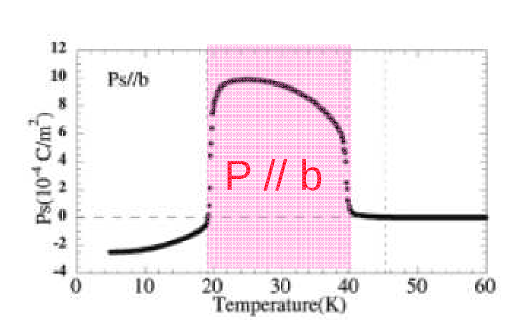

Spin-Current mechanism

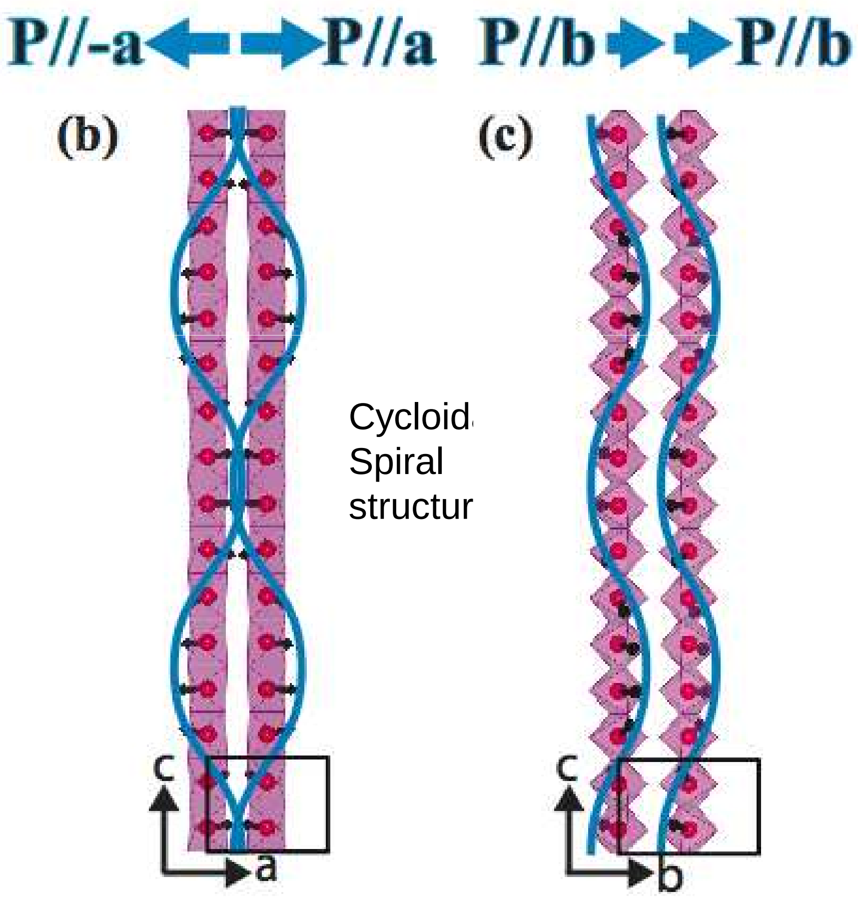

Cycloid
Spiral
structur

Magneto-Elastic mechanism

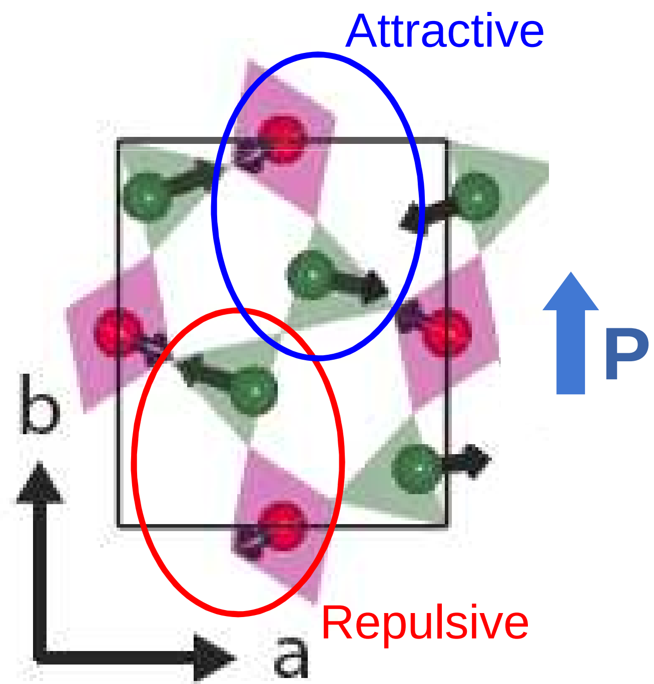

Low Temperature Incommensurate Phase (10K)

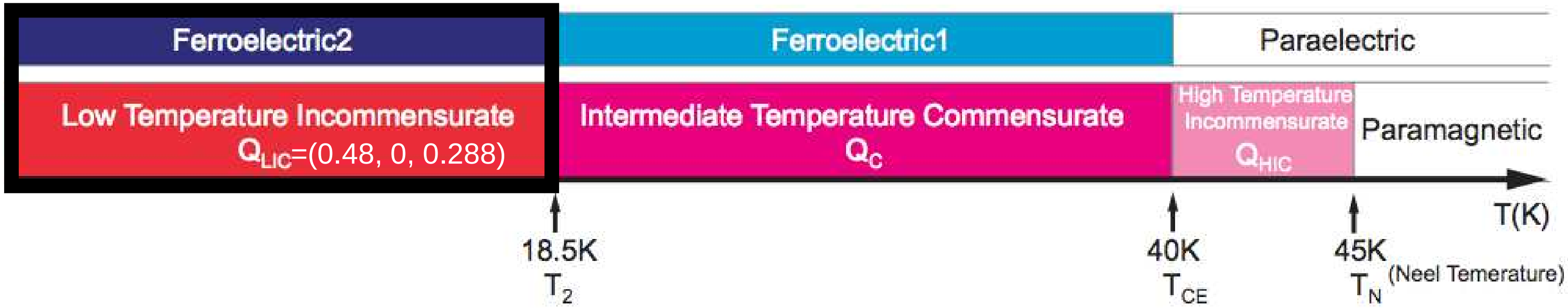

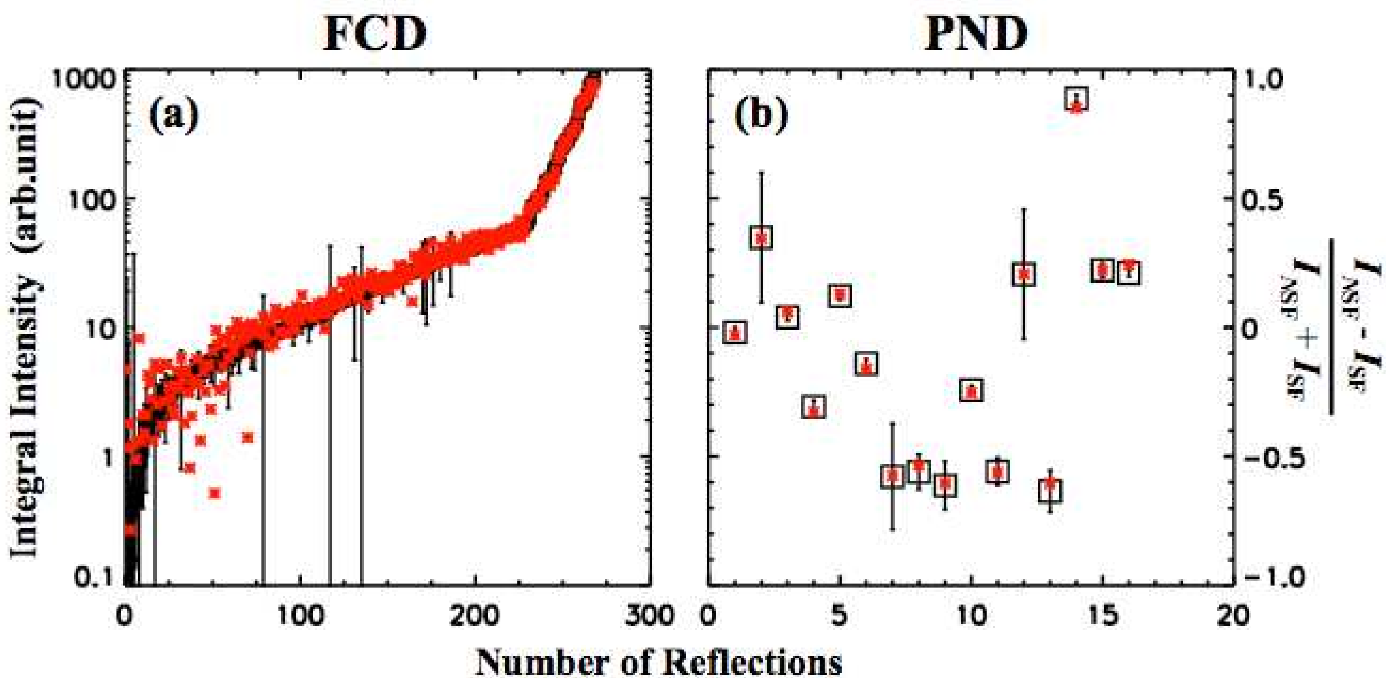

LTI (10K)

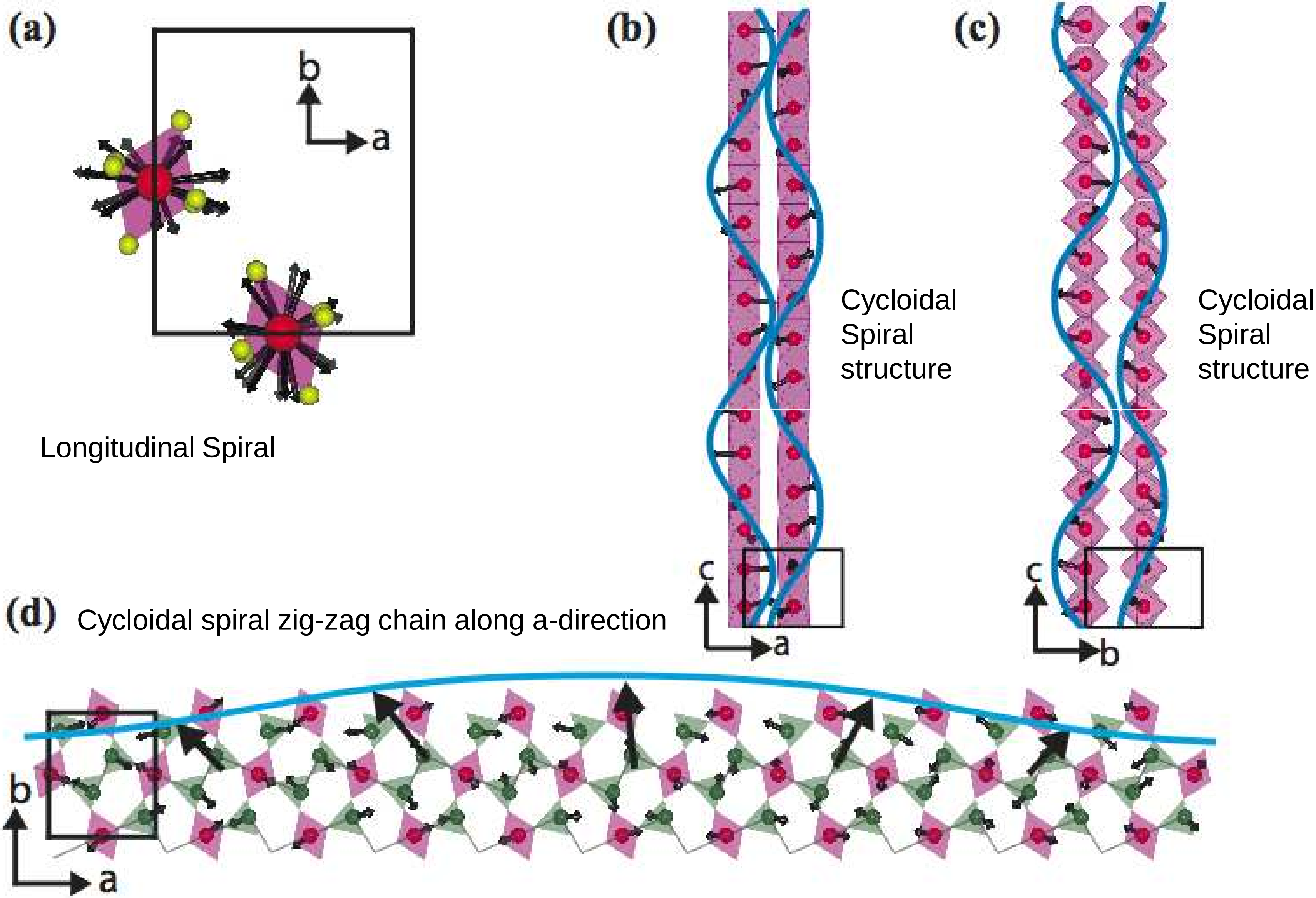

(a)
b
a
Longitudinal Spiral
(b)
Cycloidal
Spiral
structure
c
a
(c)
Cycloidal
Spiral
structure
c
b
(d)
Cycloidal spiral zig-zag chain along a-direction
b
a

YMn_2O_5

L.C. Chapon *et al. PRL* **96**, 097601 (2006)

Neutron powder diffraction

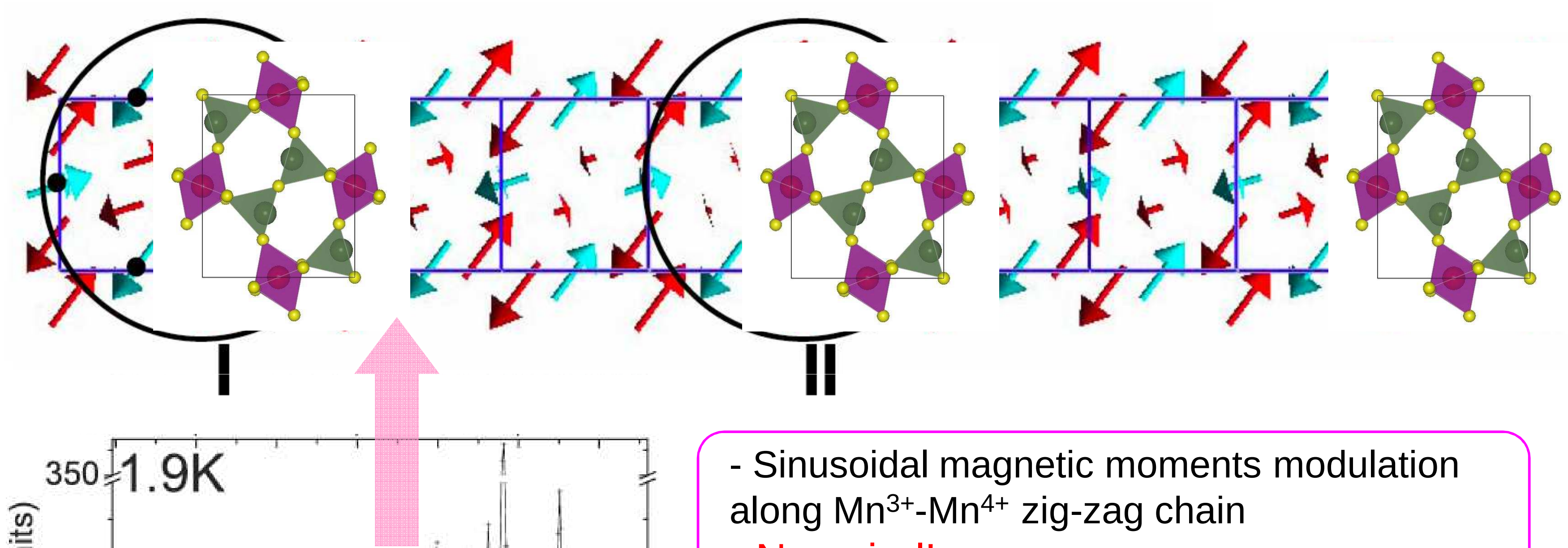

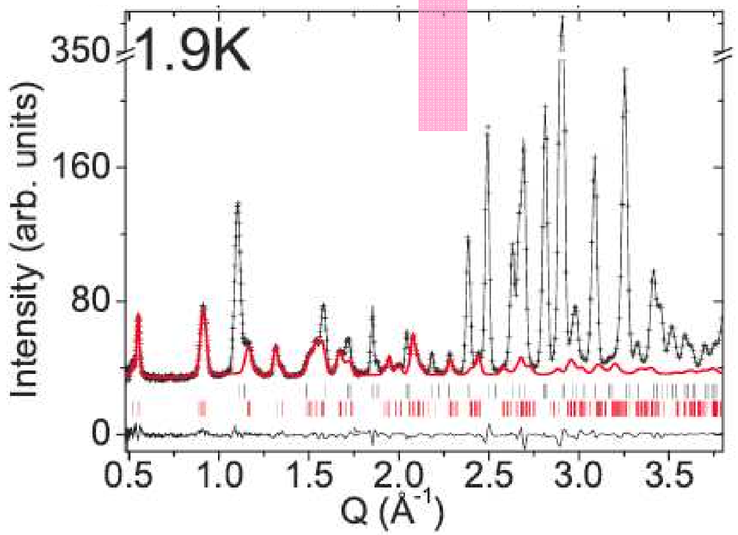

- Sinusoidal magnetic moments modulation along Mn^{3+}-Mn^{4+} zig-zag chain
- No spiral!

LTI (10K)

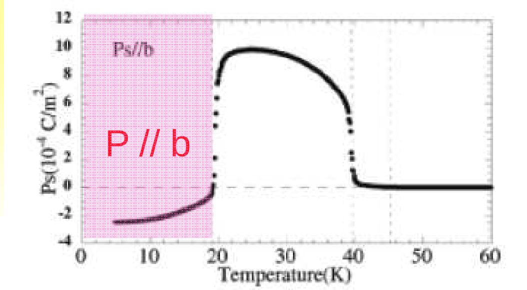

Spin-Current mechanism

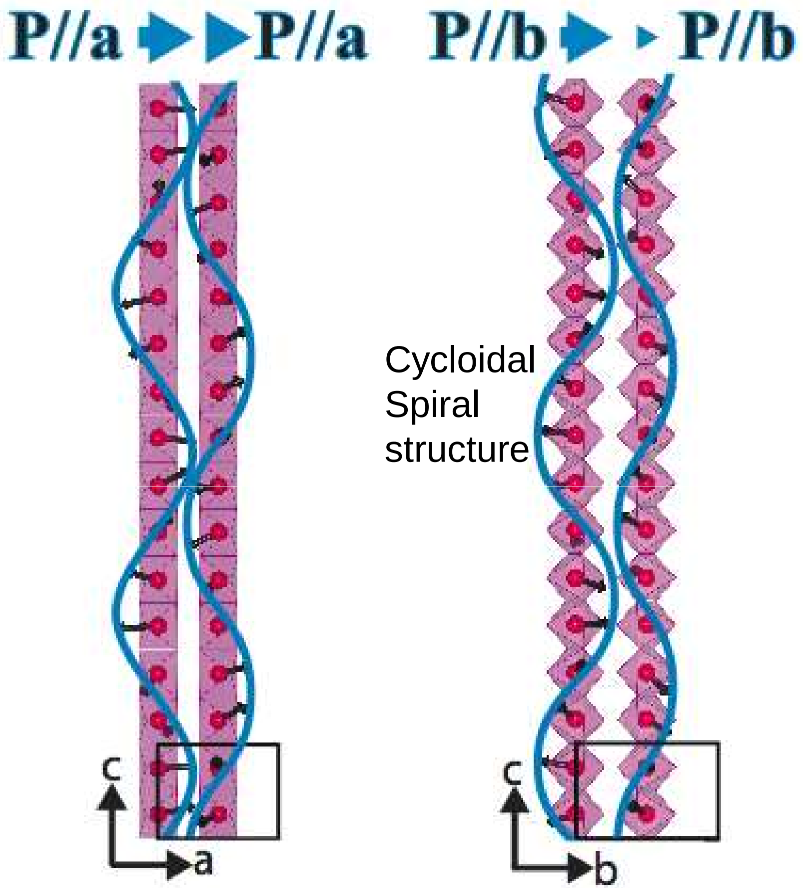

Magneto-Elastic mechanism

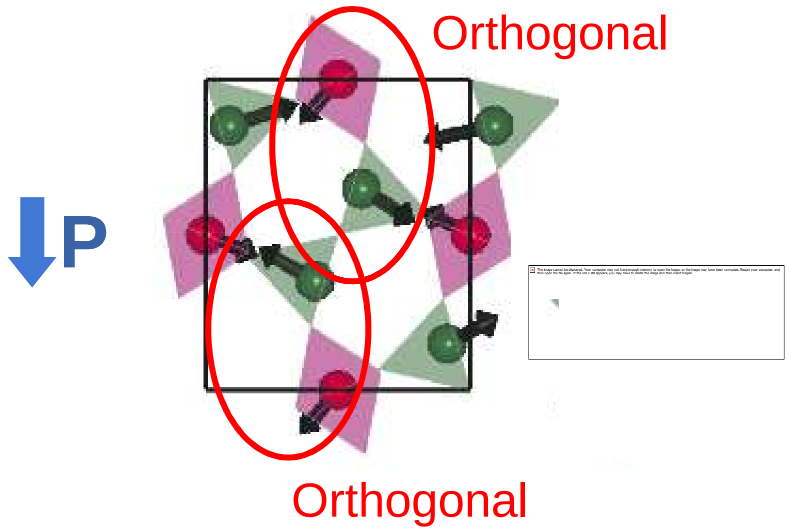

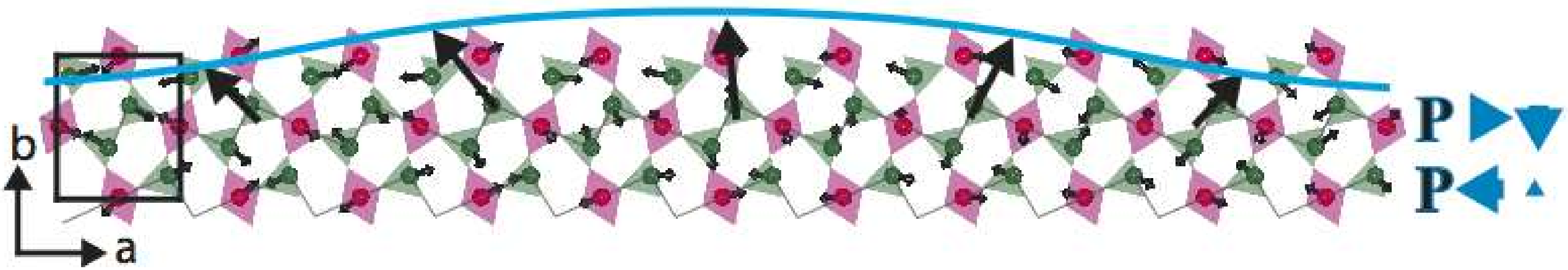

Elastic and inelastic neutron scattering

Elastic and inelastic neutron scattering can provide crucial information regarding the nature of the magneto-electric coupling by determining the magnetic structure and the effective spin Hamiltonian, respectively. We have performed the following measurements.

✓Determination of spin structure

: neutron diffraction

polarized neutron scattering (determine the axis of magnetic moments precisely)

✓ Identification of magnetic interactions: Spin Hamiltonian

: inelastic neutron scattering

Spin wave calculation of YMn_2O_5 (4 K)

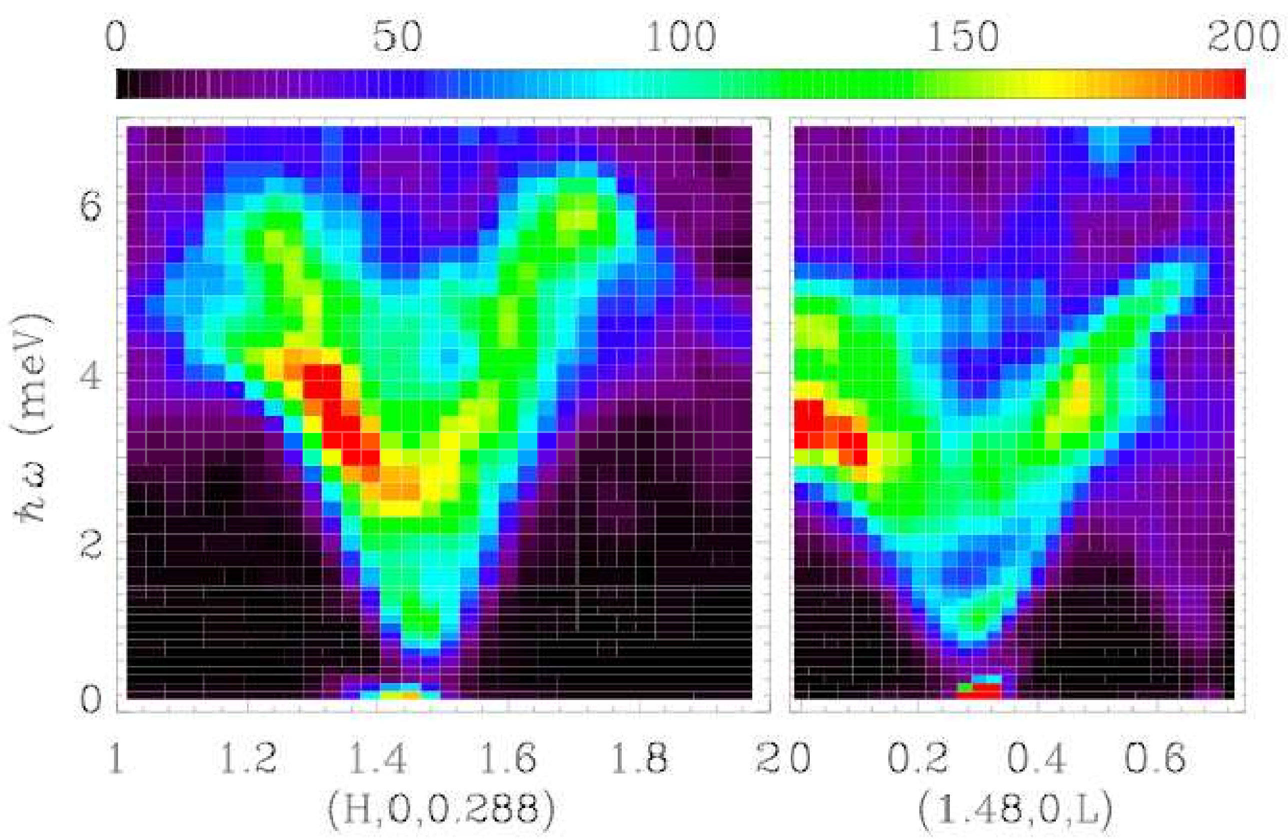

Nearest-Neighbor Magnetic Interactions

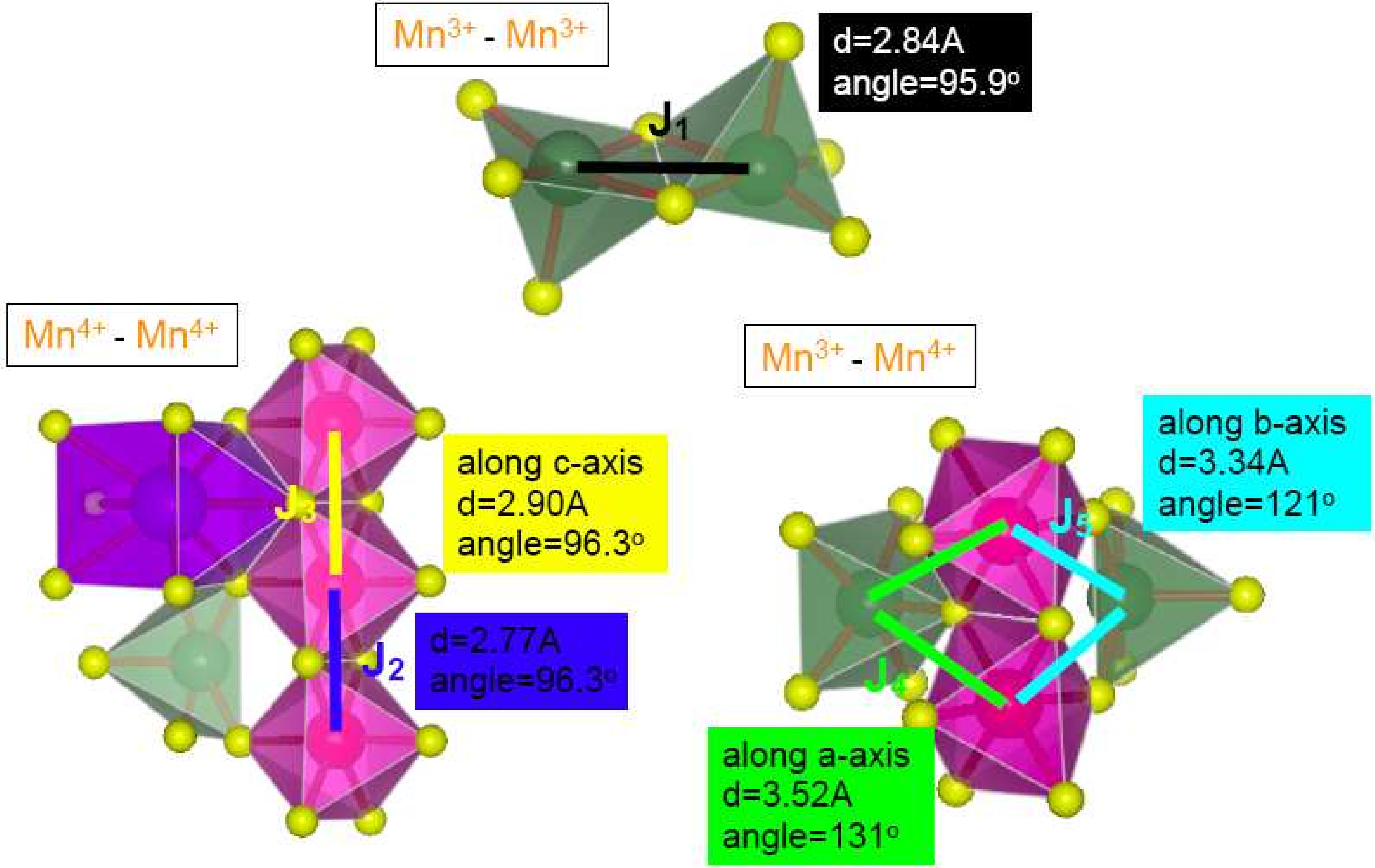

Spin wave calculation of YMn_2O_5 (4 K)

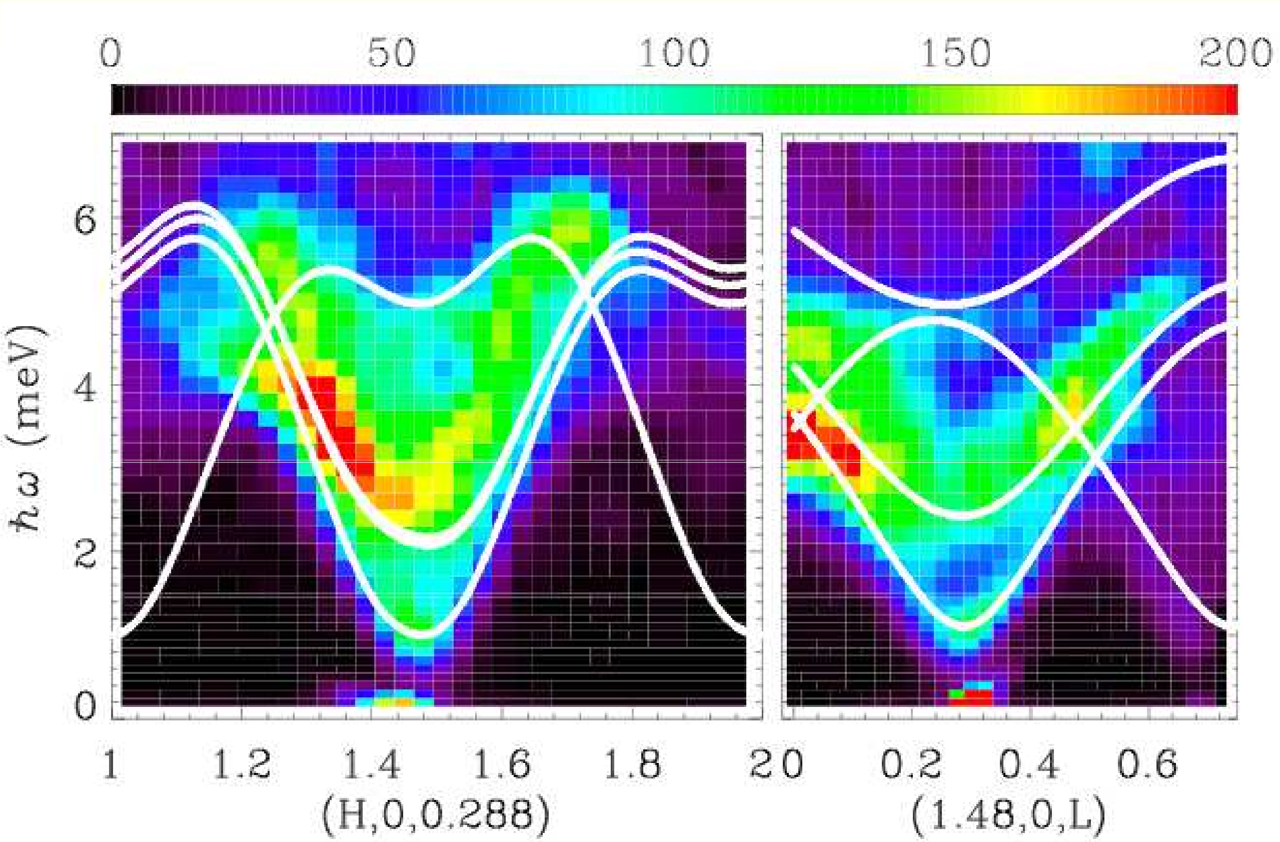

J_1 = 3.8, J_2= 0.76, J_3= -0.49, J_4= 4.56, J_5= 1.29 and D= 1.16 (unit : meV).

Conclusion

- The magnetic structures in the intermediate temperature commensurate and low temperature incommensurate phase of YMn_2O_5 have been determined by unpolarized and polarized neutron diffraction.
- The electric polarization in YMn_2O_5 can be explained by both spin-current and magneto-elastic mechanism.
- We are in the process of analyzing the data to construct the effective spin Hamiltonian in YMn_2O_5.

ITC (25K)

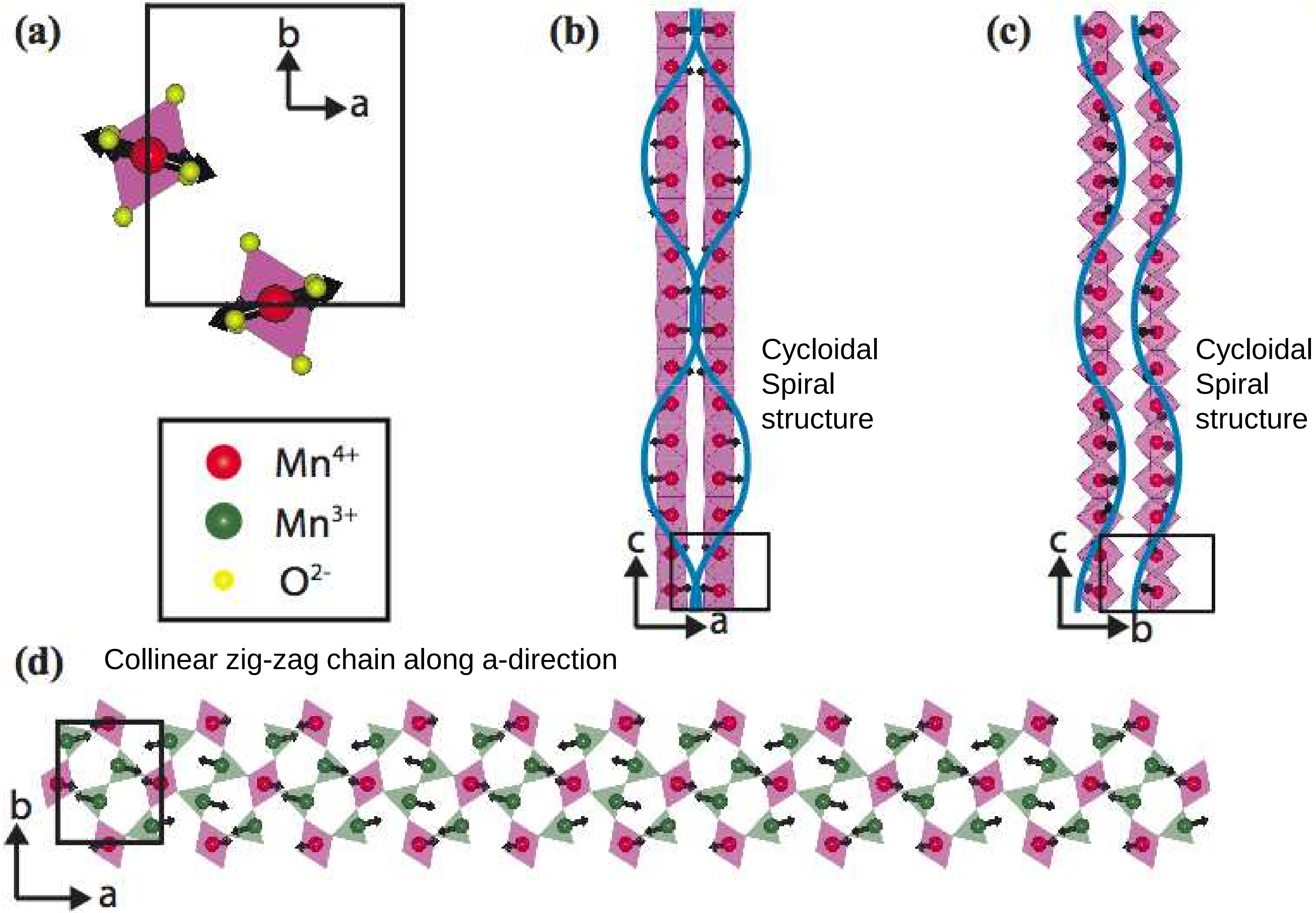

(a)
b
a
Mn4+
Mn3+
O2-
(b)
Cycloidal
Spiral
structure
c
a
(c)
Cycloidal
Spiral
structure
c
b
(d)
Collinear zig-zag chain along a-direction
b
a

Entanglements

Consider a spin pair of $s_i = 1/2$

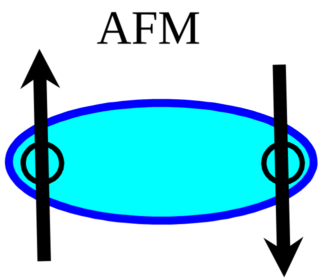

Entangled states

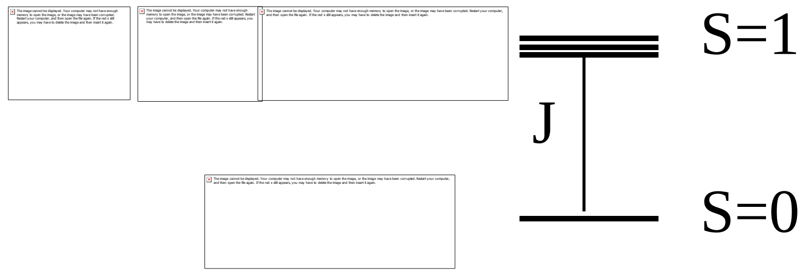

Magnetic excitations of Quantum dimer on triangular lattice : $Ba_3Cr_2O_8$

Crystal structure of $Ba_3Cr_2O_8$

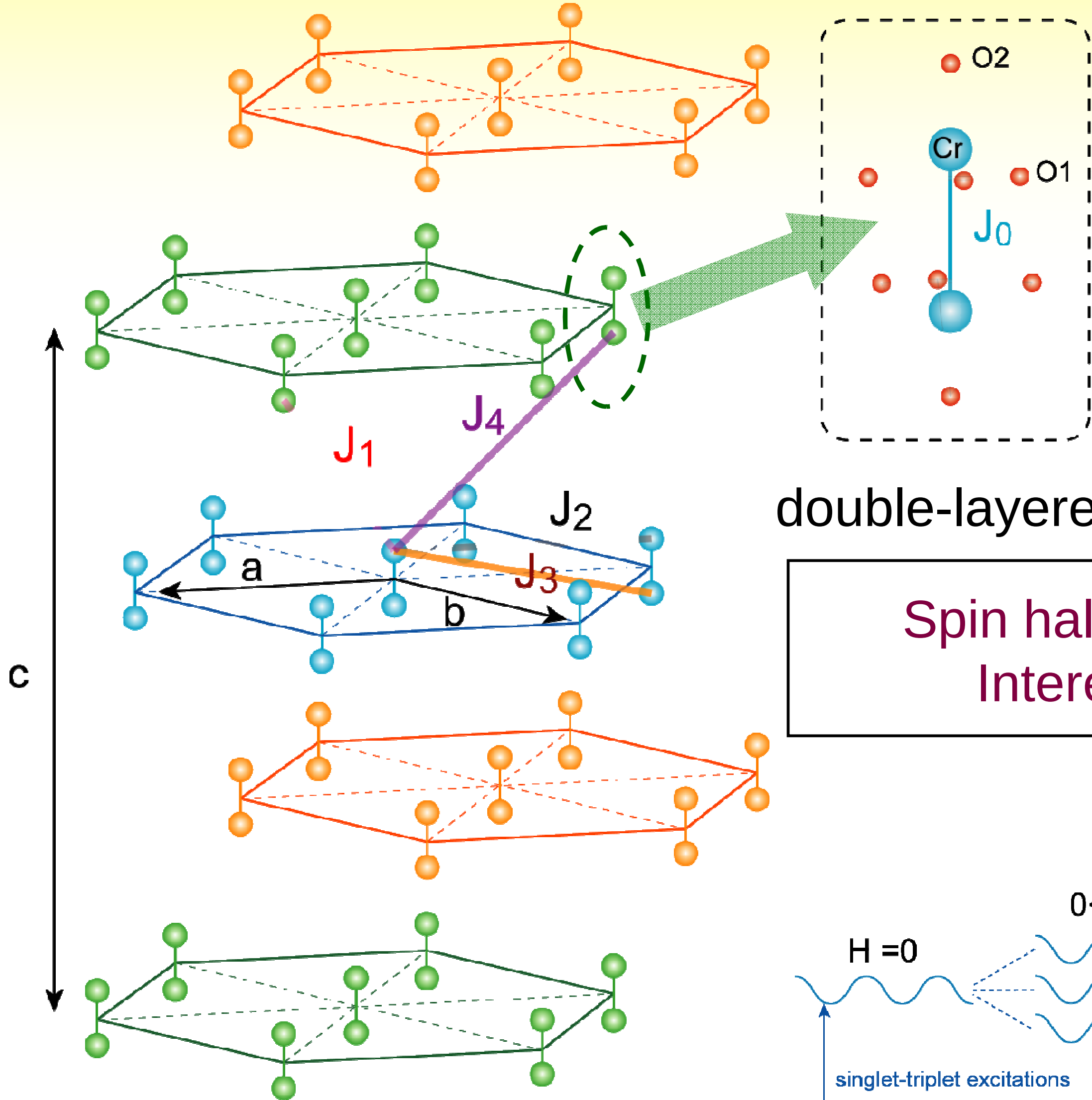

Space group : $R\bar{3}m$

Cr^{5+} : $3d^1$ ($e_g^{\,1}$), s=1/2

isolated CrO_4 tetrahedral

double-layered hexagonal plane

Spin half +dimer+triangular lattice
Interest for BEC of magnon

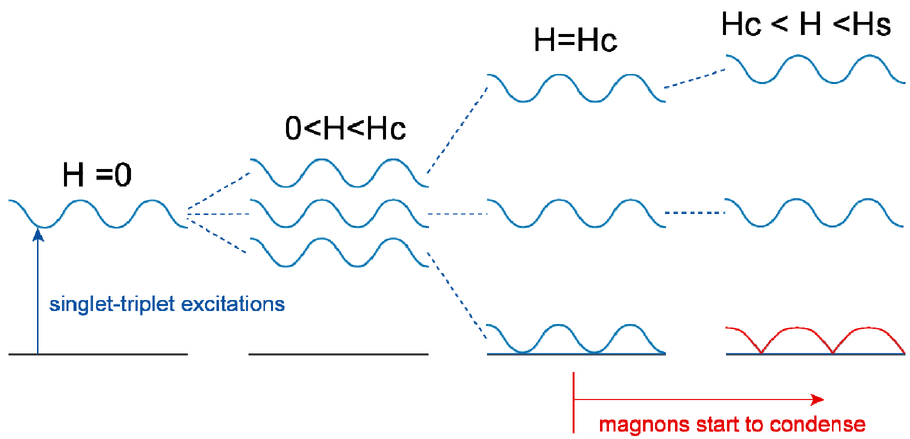

M. Kofu *et al. PRL* **102**, 037206 (2009)

Experimental methods

• Powder (17g from Y. Ueda group) and single crystal samples (0.45g) were used.

• Neutron scattering

Triple-Axis Spectroscopy : **SPINS** at NCNR (USA)

Time-Of-Flight Spectroscopy : **DCS** at NCNR (USA)

SPINS **DCS**

Magnetic excitations

(a) T = 1.7K

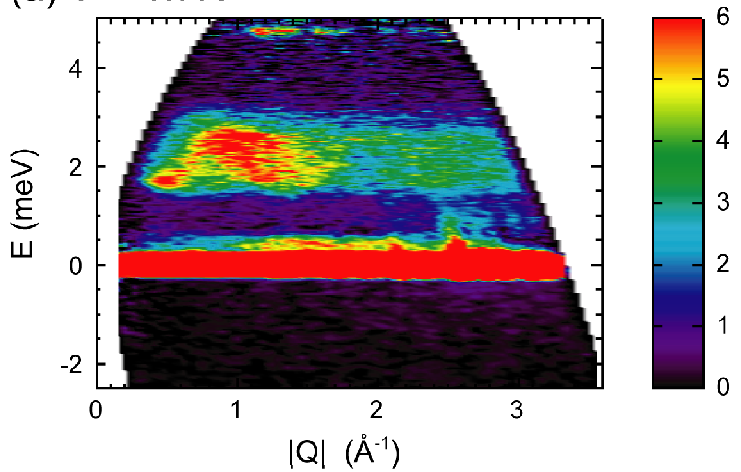

-Magnetic excitations appear only around 2meV.

- singlet-triplet excitations

- centered at J_0 ~ 2.2 meV
  gap energy D ~ 1.5 meV

(b) T = 25K

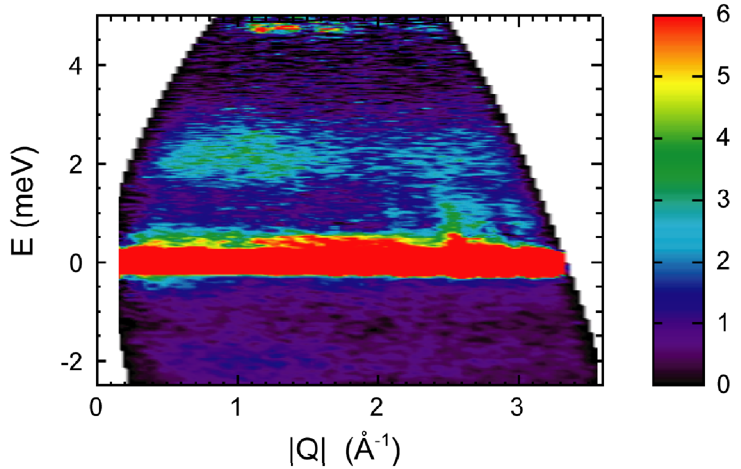

(d) T = 90K

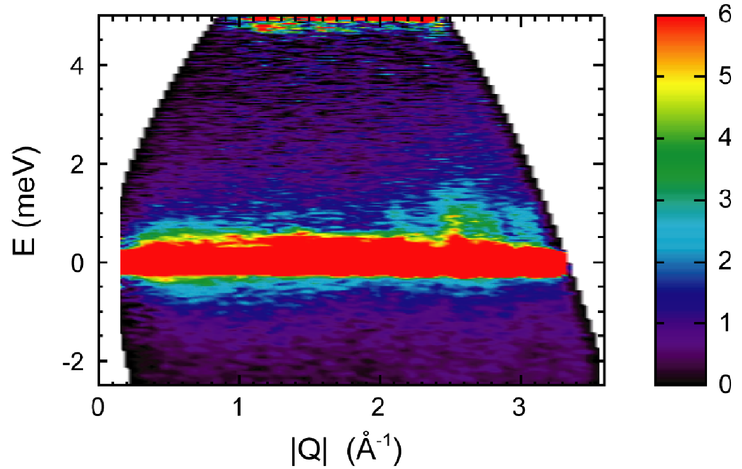

Magnetic excitations

Single crystal scattering

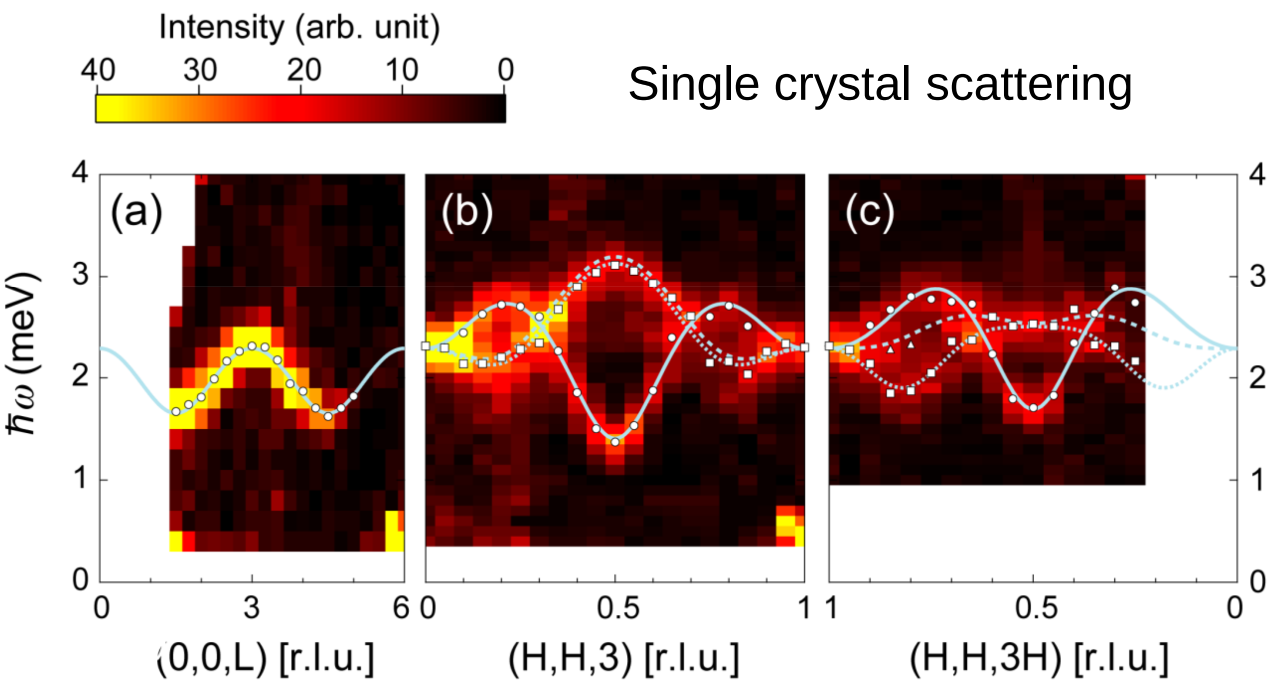

Magnetic excitations in $Ba_3Mn_2O_8$ (s=1 dimer system)

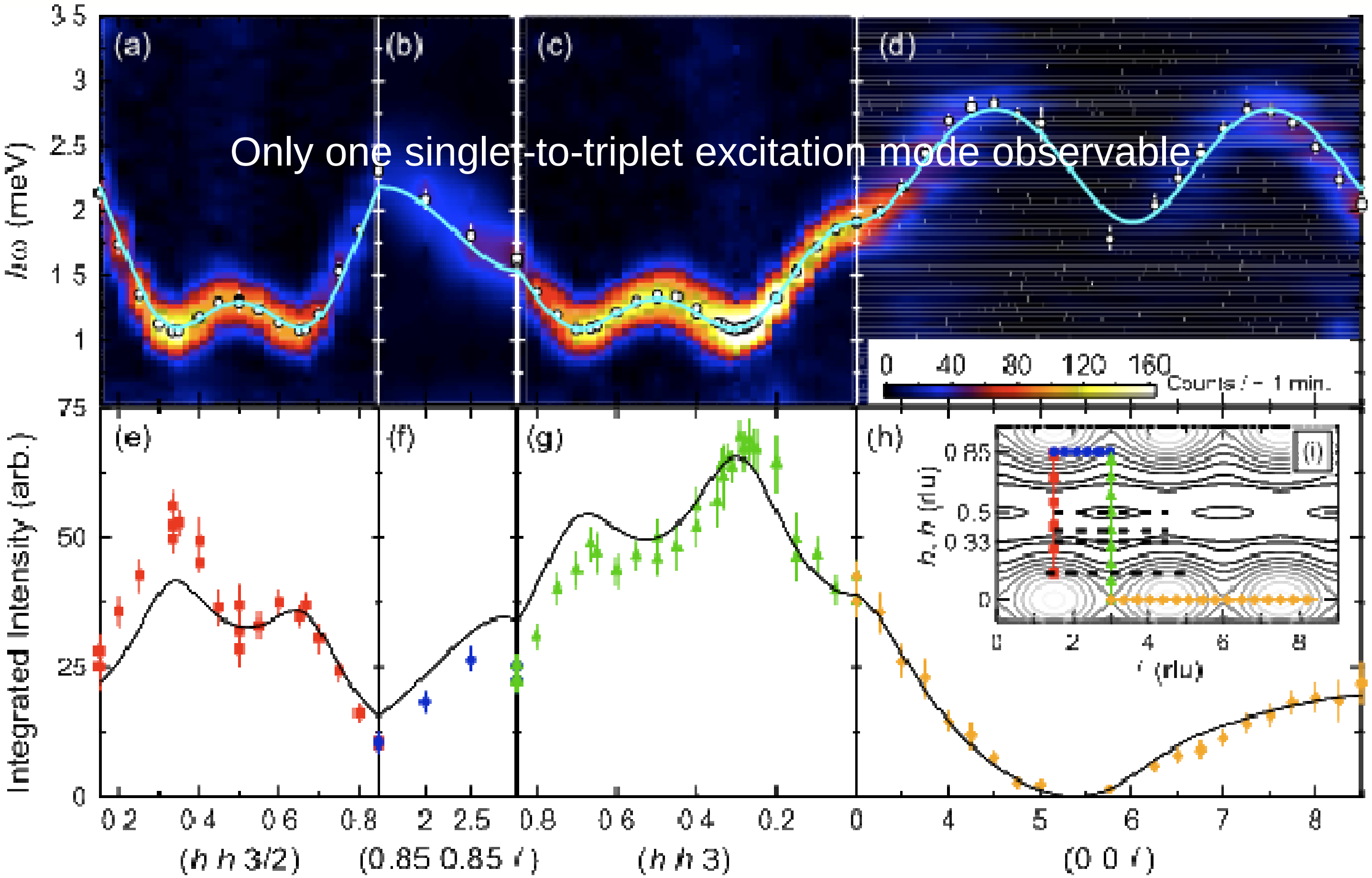

J=-1.64meV
J_c=0.12meV
J_p=-0.11meV

M. B. Stone *et al. PRL* **100**, 237201 (2008)

Magnetic excitations of $Ba_3Cr_2O_8$

Single crystal scattering

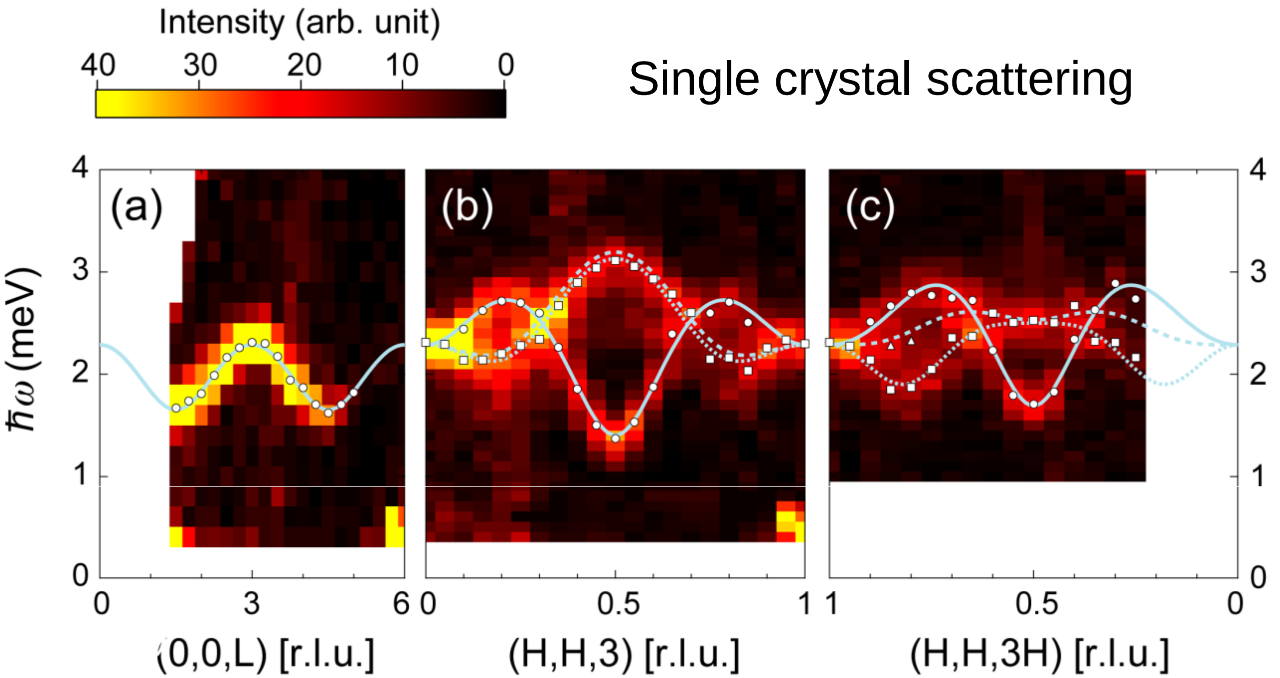

Why are multiple modes observed?

The origin of multiple modes

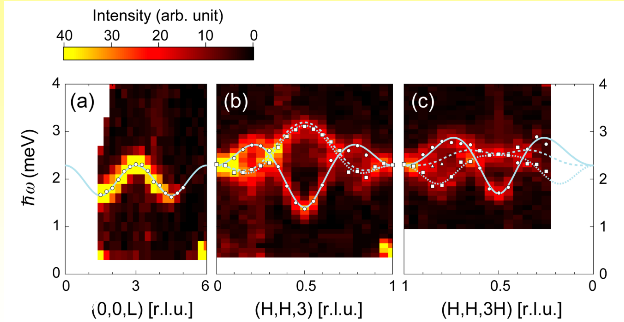

1. Is one triply degenerate mode split into three modes? NO!
2. Are there one acoustic and two optical modes?

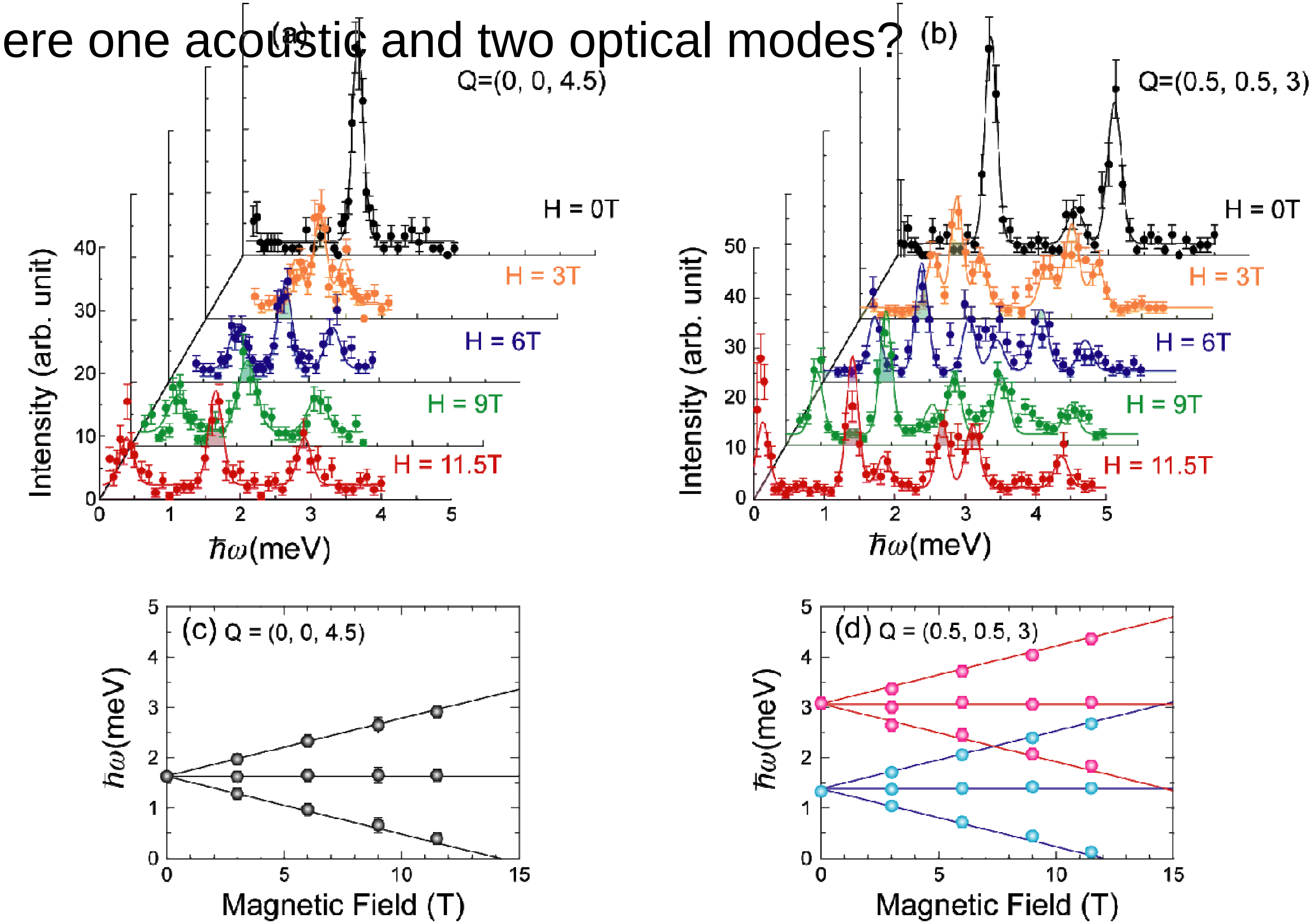

$Cs_3Cr_2Br_9$ (s=3/2 dimer system)

B. Leuenberger *et al*. (PRB **30**, 6300 (1984)) observed an optical magnon mode in $Cs_3Cr_2Br_9$ where Cr^{3+} ions form two bilayer triangular planes.

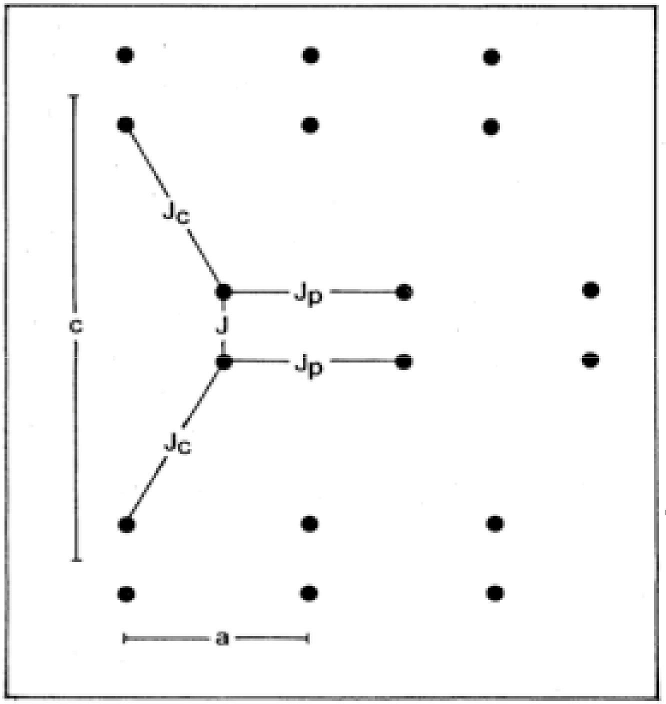

$J = -1.03(1)$ meV ,

$J_p = -0.054(1)$ meV ,

$J_c = -0.039(1)$ meV .

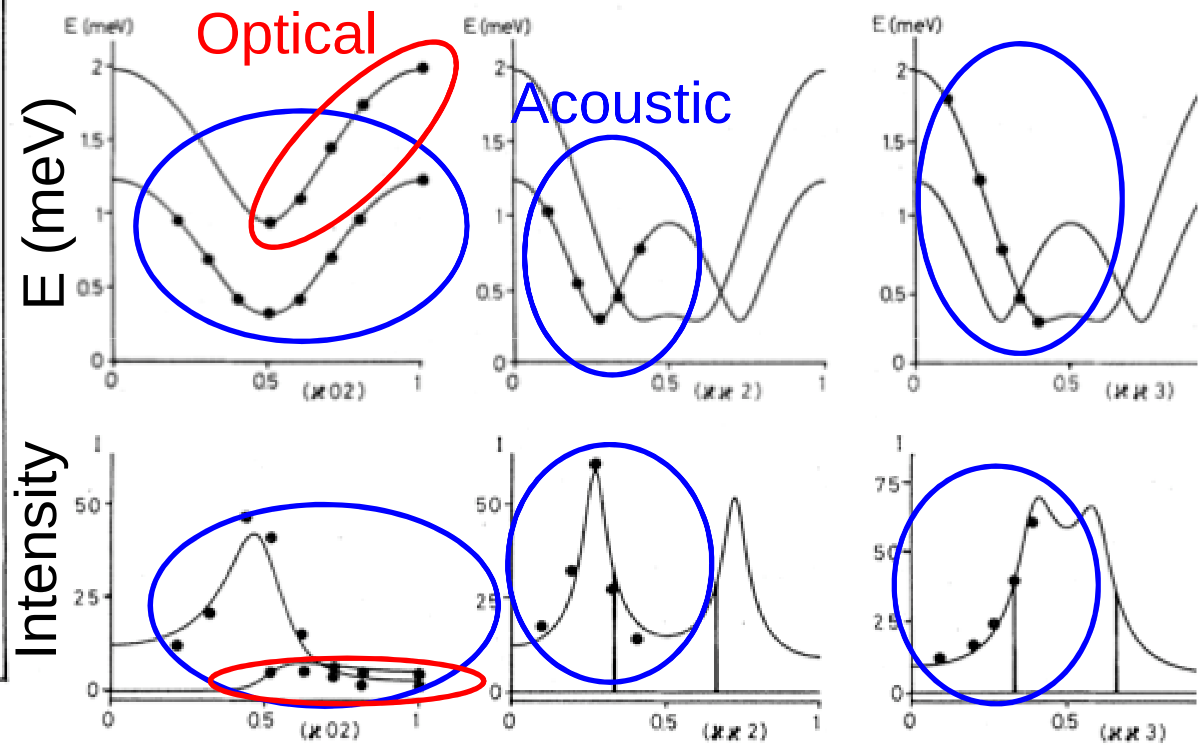

$$\omega^{\text{acoustic/optic}}(\vec{q}) = [J^2 + M^2 J (n_0 - n_1)(J_p \gamma_p(\vec{q}) \mp J_c \,|\gamma_c(\vec{q})|\,)]^{1/2} \,.$$

The origin of multiple modes

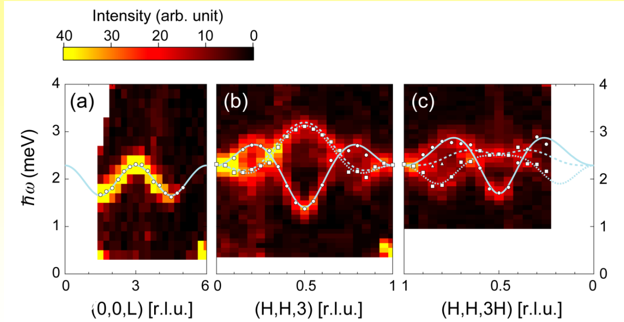

1. Is one triply degenerate mode split into three modes? NO!
2. Are there one acoustic and two optical modes? NO!

$$\left(\frac{d^2\sigma(\vec{\kappa},\omega)}{d\Omega dE'}\right)_{\text{inelatic}} \sim F(\vec{\kappa})^2(1-e^{-\hbar\omega/kT})^{-1}(n_0-n_1)(-J)\left(1-\cos(\vec{\kappa}\cdot\vec{R})\right)$$
$$\times\left[(1+2\cos(\vec{\rho}\cdot\vec{\tau}))\frac{\delta\left(\omega-\omega^{\text{acoustic}}(\vec{q})\right)}{\omega^{\text{acoustic}}(\vec{q})}\right.$$
$$\left.+(1-\cos(\vec{\rho}\cdot\vec{\tau}))\left\{\frac{\delta\left(\omega-\omega^{\text{optic}_1}(\vec{q})\right)}{\omega^{\text{optic}_1}(\vec{q})}+\frac{\delta\left(\omega-\omega^{\text{optic}_2}(\vec{q})\right)}{\omega^{\text{optic}_2}(\vec{q})}\right\}\right]$$

$$\begin{pmatrix}\omega^{\text{acoustic}}(\vec{q})\\ \omega^{\text{optic}_1}(\vec{q})\\ \omega^{\text{optic}_2}(\vec{q})\end{pmatrix}=\begin{pmatrix}\sqrt{J^2+J(n_0-n_1)(J_p\gamma_p(\vec{q})+2J_c|\gamma_c(\vec{q})|\cos\phi)}\\ \sqrt{J^2+J(n_0-n_1)(J_p\gamma_p(\vec{q})-2J_c|\gamma_c(\vec{q})|\cos(\phi-\frac{\pi}{3}))}\\ \sqrt{J^2+J(n_0-n_1)(J_p\gamma_p(\vec{q})-2J_c|\gamma_c(\vec{q})|\cos(\phi+\frac{\pi}{3}))}\end{pmatrix}$$

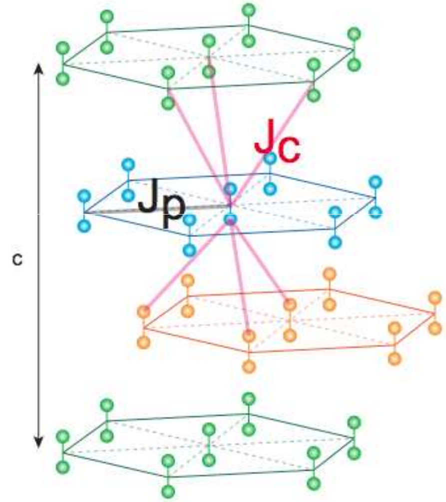

: vector between sublattice, ***J*** : interaction between a dimer

: reciprocal lattice vector

$\Rightarrow$ No optical mode can be observed

The origin of multiple modes

3. Are there spatially anisotropic interdimer interactions?

Cr^{5+} : $3d^1$ ($e_g^{\,1}$), s=1/2

Cf) Mn^{5+} : $3d^2$ ($e_g^{\,2}$), s=1

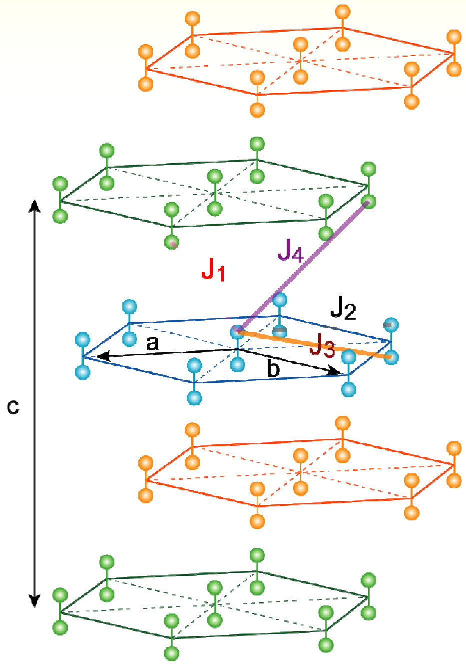

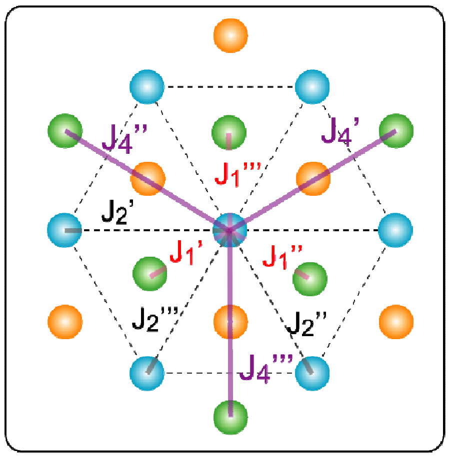

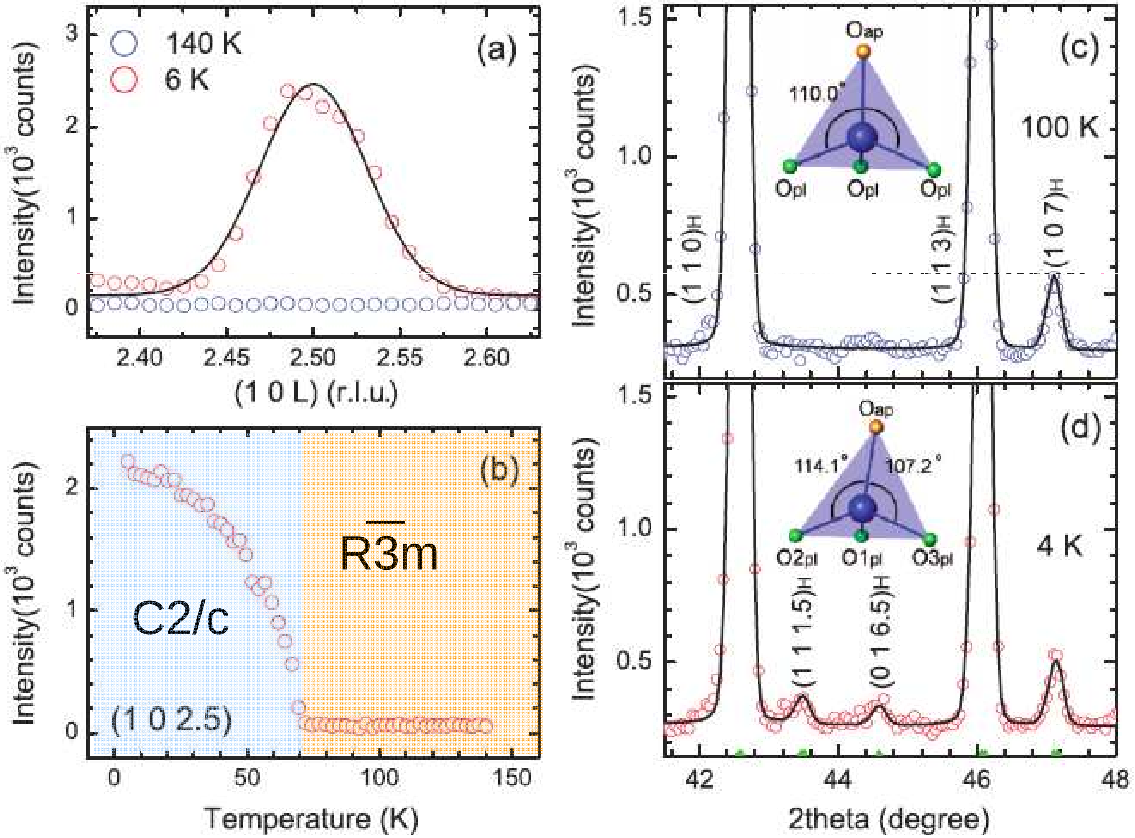

Spatially anisotropic interdimer interactions

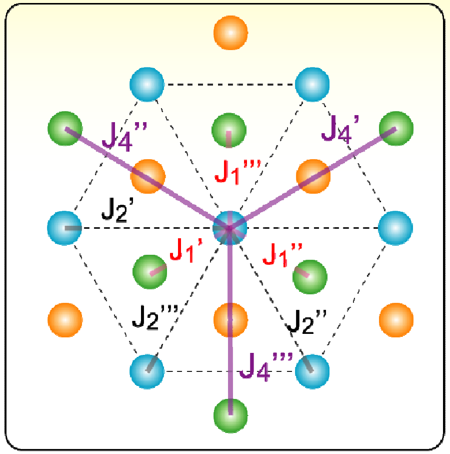

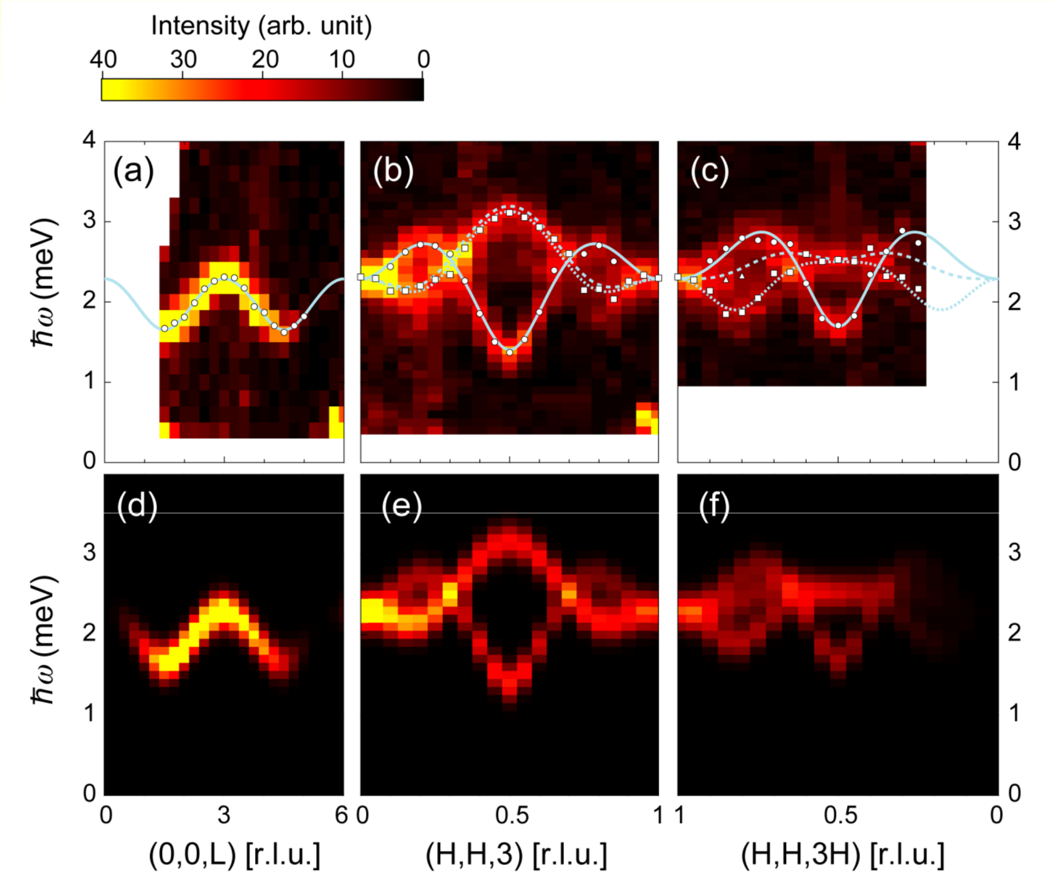

$$\left(\frac{d^2\sigma(\vec{\kappa},\omega)}{d\Omega dE'}\right)_{\text{inelatic}} \sim \frac{F(\vec{\kappa})^2\left(1-\cos(\vec{\kappa}\cdot\vec{R})\right)}{\hbar\omega(\vec{\kappa})}$$

$$\hbar\omega(\vec{q}) = \sqrt{J^2 + J\gamma(\vec{q})},$$

$$\gamma(\vec{q}) = \sum_i J_{\text{inter}}(\vec{R}_i)\exp^{-i\vec{q}\cdot\vec{R}_i}$$

J_0=2.38meV

J_1'=0.08	J_2'=0.10	J_4'=0.04
J_1''=-0.15	J_2''=0.07	J_4''=0.10
J_1'''=0.10	J_2'''=-0.52	J_4'''=0.09

Conclusion

- Spin excitations are located at 2.2 meV (center) with 1 meV bandwidth.
- Multiple excitation modes can be explained by spatially anisotropic J model.

Thanks for your attention !!

Landau theory with $TbMnO_3$

Space group : *Pbnm*

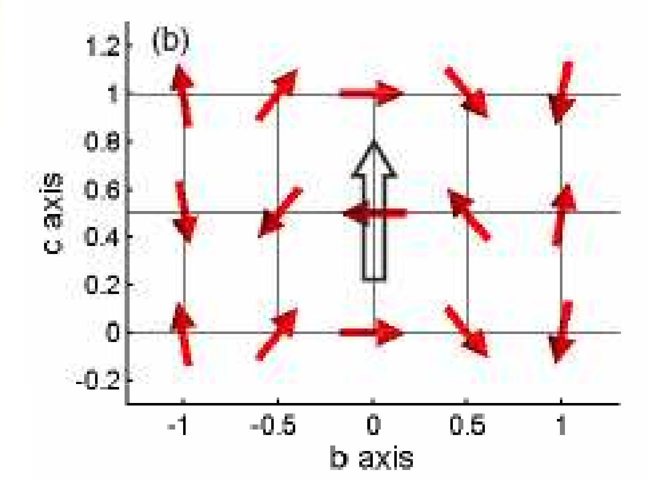

(c)

	1	2_y	m_{xy}	m_{yz}
Γ_1	1	1	1	1
Γ_2	1	1	-1	-1
Γ_3	1	-1	1	-1
Γ_4	1	-1	-1	1
P	e	o	o	e

$$\Sigma_\gamma b_\gamma \sigma_2(k)\sigma_3(-k)P_\gamma + \text{c.c.}$$

2_y : (x,y,z) $\rightarrow$(-x, -y, z)
m_{xy} : (x,y,z) $\rightarrow$(x, y, -z)
m_{yz} : (x,y,z) $\rightarrow$(-x, y, z)

P // z-direction

Geometric frustration

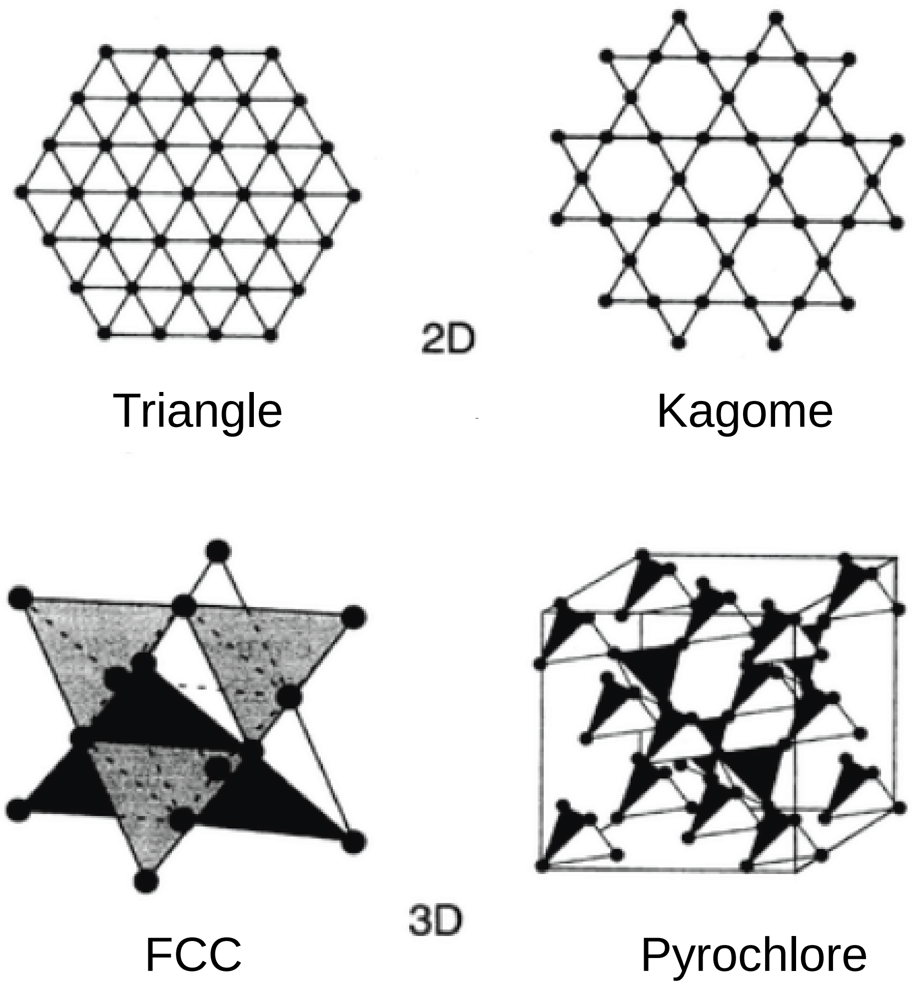

J. E. Greedan, J.Mater. Chem **1**, 37 (2001)

Triangular lattice

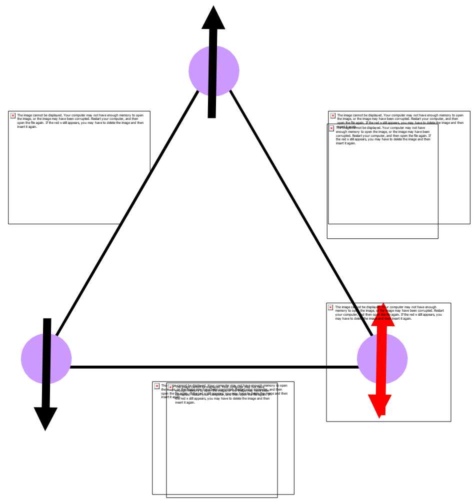

Frustrated